

Improving missing transverse momentum estimation with a deep neural network

A. Hayrapetyan *et al.**
(CMS Collaboration)

 (Received 15 September 2025; accepted 20 March 2026; published 21 April 2026)

At hadron colliders, the net transverse momentum of particles that do not interact with the detector (missing transverse momentum, \vec{p}_T^{miss}) is a crucial observable in many analyses. In the standard model, \vec{p}_T^{miss} originates from neutrinos. Many beyond-the-standard-model particles, such as dark matter candidates, are also expected to leave the experimental apparatus undetected. This paper presents a novel deep neural network based \vec{p}_T^{miss} estimator, DeepMET, developed by the CMS Collaboration at the LHC. The DeepMET algorithm produces a weight for each reconstructed particle based on its properties. The estimator is based on the negative vector sum of the weighted transverse momenta of all reconstructed particles in an event. Compared with other estimators currently employed by CMS, DeepMET improves the \vec{p}_T^{miss} resolution by 10%–30%, shows improvement for a wide range of final states, is easier to train, and is more resilient against the effects of additional proton-proton interactions accompanying the collision of interest.

DOI: [10.1103/c4z7-tqvc](https://doi.org/10.1103/c4z7-tqvc)

I. INTRODUCTION

At the CERN LHC, experiments, such as CMS [1] and ATLAS [2], use reconstruction algorithms that estimate the four-momentum, production vertex, and types of all final-state particles to extract the maximum information from the high energy proton-proton (pp) collision data. The reconstructed particles consist of muons, electrons, and photons, as well as charged and neutral hadrons, which are then clustered into jets that are the experimental signatures of energetic quarks, gluons, and tau leptons. The presence of particles that do not interact with the detector, such as standard model (SM) neutrinos or new electrically neutral, weakly interacting particles, e.g., dark matter particles, can only be inferred indirectly, by measuring the so-called missing transverse momentum, denoted as \vec{p}_T^{miss} , with magnitude p_T^{miss} . At a hadron collider, the component transverse to the beam direction of the net momentum of the initial-state partons is close to zero. The negative of the vector sum of all reconstructed particles' transverse momenta therefore estimates \vec{p}_T^{miss} ,

$$\vec{p}_T^{\text{miss}} = - \sum_{i \in \text{all reco}} \vec{p}_{T,i}. \quad (1)$$

*Full author list given at the end of the article.

Published by the American Physical Society under the terms of the [Creative Commons Attribution 4.0 International license](https://creativecommons.org/licenses/by/4.0/). Further distribution of this work must maintain attribution to the author(s) and the published article's title, journal citation, and DOI. Funded by SCOAP³.

The \vec{p}_T^{miss} stemming from weakly interacting particles will be collectively referred to as “genuine \vec{p}_T^{miss} ” in what follows. The accuracy of the \vec{p}_T^{miss} estimate is affected by the particle reconstruction efficiencies and p_T resolutions, detector finite coverage and noise, and the ability of the reconstruction algorithm to include particles from the leading pp interaction, while rejecting the potentially large number of low-momentum particles from additional pp interactions in the same or nearby bunch crossings (pileup). These factors collectively make it challenging to measure \vec{p}_T^{miss} with high accuracy and resolution. Pileup mitigation algorithms have been adopted and optimized in CMS that are effective in reducing this contribution to \vec{p}_T^{miss} resolution [3–5].

The complexity of the \vec{p}_T^{miss} measurement suggests that modern machine-learning (ML) techniques could yield a more accurate estimator. The CMS Collaboration has done previous work showing the utility of this approach. An estimator that is based on multivariate analysis (MVA) technique using boosted decision trees, referred to as MVA- \vec{p}_T^{miss} [6], is employed in CMS Run-1 analyses and demonstrates a relative improvement in precision of around 20% compared with a more traditional calculation [7], particularly for the $H \rightarrow \tau\tau$ process. However, because MVA- \vec{p}_T^{miss} was trained on specific physics processes and their global event properties, it does not, in general, have optimal performance for other physics processes and kinematic regions.

This paper introduces a new algorithm DeepMET based on a deep neural network (DNN). For each reconstructed particle in the event, the DNN produces a unique weight based on the properties of the particles. The DeepMET \vec{p}_T^{miss}

estimator is based on the negative of the vector sum of the weighted transverse momenta of all particles in an event. In this paper, we describe DeepMET and compare its performance to that of other \vec{p}_T^{miss} estimators. Our performance metrics are based on the response and resolution for the x and y components of a \vec{p}_T^{miss} estimator, the components parallel and perpendicular to the transverse direction of a Z boson (for samples enriched in this process), or the absolute value of p_T^{miss} . The response is defined as the ratio of the measured average to the true average. The response can be smaller than unity due to e.g., particles below reconstruction thresholds or the response of the calorimeters. It can be larger due to resolution effects, noise, and pileup. The resolution can be calculated both with and without correction for the response. Since it can be difficult to know the true \vec{p}_T^{miss} in an event, artificial \vec{p}_T^{miss} can be induced in events with little to no genuine \vec{p}_T^{miss} by excluding leptons from the \vec{p}_T^{miss} calculation (e.g., the muons in a $Z \rightarrow \mu\mu$ event) and comparing with the corresponding precisely measured quantity calculated from the leptons.

Compared with conventional \vec{p}_T^{miss} estimators, DeepMET shows a relative improvement in the \vec{p}_T^{miss} resolution of 10%–30%, and is more resilient to the effects of pileup. Due to the choice of DNN architecture and its inputs, i.e., the usage of reconstructed particles and the exclusion of event-level observables, the algorithm has limited information about the event topology and is trained only with typical pp events. As a consequence, DeepMET is trained quickly and generalizes well, showing similarly strong performance in both collision data and a diverse set of simulated physics processes.

The paper is structured as follows. Section II gives an overview of the CMS detector. In Sec. III, a summary of existing algorithms is presented, along with their strengths and weaknesses. Sections IV and V contain details of the datasets and the object and event selections. After a brief introduction to the \vec{p}_T^{miss} parametrization, Sec. VI details the algorithm, its inputs and outputs, and the associated loss functions. Performance metrics and comparisons with alternative algorithms are discussed in Sec. VII. A method to calibrate simulation performance to align with real collision data is outlined in Sec. VIII. Section IX explores the source of the enhanced performance of DeepMET. Benchmarks for the computational needs are given in Sec. X. Finally, a summary is presented in Sec. XI.

Tabulated results are provided in the HEPData record for the performance comparisons in this analysis [8].

II. THE CMS DETECTOR

The central feature of the CMS apparatus is a superconducting solenoid of 6 m internal diameter, providing a magnetic field of 3.8 T. Within the solenoid volume are a silicon pixel and strip tracker, a lead tungstate crystal

electromagnetic calorimeter (ECAL), and a brass and scintillator hadron calorimeter (HCAL), each composed of a barrel and two end cap sections. Forward hadron (HF) calorimeters extend the pseudorapidity (η) coverage to high values ($|\eta| \leq 5$) assuring very good hermeticity. Muons are detected in gas-ionization detectors embedded in the steel flux-return yoke outside the solenoid. A more detailed description of the CMS detector, together with a definition of the coordinate system used and the relevant kinematic variables, is reported in Ref. [1].

Events of interest are selected using a two-tiered trigger system. The first level, composed of custom hardware processors, uses information from the calorimeters and muon detectors to select events of interest at a rate of around 100 kHz within a fixed time interval of about 4 μ s [9]. The second level, known as the high-level trigger, consists of a farm of processors running a version of the full event reconstruction software optimized for fast processing, and reduces the event rate to $\mathcal{O}(1 \text{ kHz})$ before data storage [10,11].

III. RECONSTRUCTION, PILEUP MITIGATION, AND MACHINE LEARNING

A. Particle-flow reconstruction

Primary collision vertices (PVs) corresponding to pp collisions are found using reconstructed charged particles [12]. The primary pp interaction vertex corresponding to the hardest scattering in the event, evaluated using tracking information alone, is referred to as the leading primary vertex (LPV), as described in Sec. 9.4.1 of Ref. [13]. Other PVs are referred to as pileup vertices.

A particle-flow (PF) algorithm [14] aims to reconstruct and identify each individual particle in an event, using an optimized combination of information from the various elements of the CMS detector. The energy of a photon is obtained from the ECAL measurement. The energy of an electron is determined from a combination of the electron momentum at the primary interaction vertex as determined by the tracker, the energy of the corresponding ECAL cluster, and the energy sum of all bremsstrahlung photons spatially compatible with originating from the electron track. The p_T of a muon is obtained from the curvature of the corresponding track. The energy of a charged hadron is determined from a combination of the momentum measured in the tracker and the matching ECAL and HCAL energy deposits, corrected for the response function of the calorimeters to hadronic showers. Finally, the energy of a neutral hadron is obtained from the corresponding corrected ECAL and HCAL energies. The reconstructed particles from the PF algorithm are referred to as PF candidates.

Muons are measured in the range $|\eta| < 2.4$, with detection planes made using three technologies: drift tubes, cathode strip chambers, and resistive-plate chambers. The single-muon trigger efficiency exceeds 90% over the full

η range, and the efficiency to reconstruct and identify muons is greater than 96%. Matching muons to tracks measured in the silicon tracker results in a relative p_T resolution, for muons with p_T up to 100 GeV, of 1% in the barrel and 3% in the endcaps. Measurements made with cosmic ray muons show that, in the central region of the detector, the p_T resolution is better than 7% for muons with p_T up to 1 TeV [15].

For each event, hadronic jets are clustered from these reconstructed particles using the infrared and collinear safe anti- k_T algorithm [16,17] with a distance parameter of 0.4. Jet momentum is determined as the vector sum of all particle momenta in the jet, and is found from simulation to be, on average, within 5% to 10% of the true momentum over the whole p_T spectrum and detector acceptance. Jet energy corrections are derived from simulation studies so that the average measured energy of jets becomes identical to that of particle level jets. *In situ* measurements of the momentum balance in dijet, photon + jet, Z + jet, and multijet events are used to determine any residual differences between the jet energy scale (JES) in data and in simulation, and appropriate corrections are made. The jet energy resolution (JER) typically amounts to 15%–20% at 30 GeV, 10% at 100 GeV, and 5% at 1 TeV [18]. Additional selection criteria are applied to each jet to remove jets potentially dominated by instrumental effects or reconstruction failures.

The reconstruction also produces a \vec{p}_T^{miss} estimator, PF \vec{p}_T^{miss} , which is calculated using all reconstructed PF candidates in an event [19] and is further corrected for the JES of reconstructed jets. The \vec{p}_T^{miss} relies on the accurate measurement of the reconstructed physics objects, namely muons, electrons, photons, hadronically decaying taus, jets, and unclustered energy (E_U). The E_U is the contribution from the PF candidates not associated with any of the previous physics objects.

B. Pileup mitigation

Pileup affects jet and \vec{p}_T^{miss} measurements, since contributions from additional tracks and calorimetric energy depositions increase the apparent jet momentum and change the subsequent \vec{p}_T^{miss} estimation. To mitigate such effects on jets, charged-hadron subtraction (CHS) removes tracks identified as originating from pileup vertices from jets [3]. Corrections are then applied to remove on average the remaining contributions from neutral particles. This correction to the p_T of the jets is then propagated to the \vec{p}_T^{miss} estimation [18,19].

The pileup-per-particle identification algorithm (PUPPI) [3–5] can additionally be used to mitigate the effect of pileup by making use of local shape information, event pileup properties, and tracking information. Charged particles identified as originating from pileup vertices are discarded. For each neutral particle, a local shape variable, that distinguishes collinear energy deposits originating

from the hard scatter from soft/diffuse energy deposits attributable to particles originating from pileup interactions, is defined using the surrounding charged particles that are compatible with the LPV within the tracker acceptance ($|\eta| < 2.5$) and using all particles in the region outside of the tracker coverage. The momenta of the neutral particles are then rescaled according to their probability to originate from the LPV as deduced from the local shape variable. We denote this probability as the ‘‘PUPPI weight’’ in the following. The rescaling supersedes the need for jet-based offset corrections [3]. The corresponding \vec{p}_T^{miss} is referred to as PUPPI \vec{p}_T^{miss} . In the studies of this paper, ‘‘PUPPI v15’’ tune is used [5].

The CHS and PUPPI algorithms have been shown to improve the precision of \vec{p}_T^{miss} measurements significantly [19]. However, the PUPPI algorithm requires extensive tuning. Its efficacy depends both on the physics process and kinematic region, and it is less effective in low-pileup data. Consequently, its \vec{p}_T^{miss} resolution is not always optimal.

IV. DATA AND SIMULATED SAMPLES

This paper uses a data sample collected by the CMS experiment at a center-of-mass energy of 13 TeV during 2016. The dataset corresponds to an integrated luminosity of $\mathcal{L} = 16.8 \text{ fb}^{-1}$, with an average pileup of 23 additional pp interactions [20]. The DeepMET algorithm was deployed for the remainder of Run 2 and Run 3 as well, where it showed comparable performance gains.

Several Monte Carlo (MC) event generators are used to simulate the Z + jets and $t\bar{t}$ samples for the ML training and W + jets samples for the post-training performance studies. The V + jets ($V = W, Z$) samples are simulated at next-to-leading order (NLO) in perturbative quantum chromodynamics (QCD) with the MADGRAPH5_aMC@NLO2.3.3 event generator [21]. The $t\bar{t}$ samples are simulated with POWHEG2.0 [22–25]. The PYTHIA8.230 [26] package is used for parton showering, hadronization, and the underlying event simulation, with the CP5 tune [27,28]. The NNPDF 3.1 [29] set of parton distribution functions (PDFs) at next-to-NLO in QCD is used as the default.

Additional sets of simulated event samples are used to understand how the performance of the DeepMET reconstruction depends on the physical process. The processes span a variety of final states, including Higgs bosons, top quarks, heavy-flavor jets, τ leptons, and beyond-the-SM dark-matter candidates. These samples are produced using the same PDFs with the same tunes. Four types of Higgs boson processes are generated with POWHEG at NLO in perturbative QCD: Higgs boson production via vector boson fusion with the Higgs boson decaying to invisible particles ($H \rightarrow \text{invisible}$), Higgs boson pair production via gluon fusion with one Higgs boson decaying to a pair of τ leptons (τ decay inclusively) and the other Higgs boson decaying to a pair of b quarks ($HH \rightarrow b\bar{b}\tau\tau$), and Higgs bosons

TABLE I. Overview of the simulated event samples used for performance studies.

Process	Production mode, decay chain	Final-state objects
<i>Standard model</i>		
Z boson	$Z + \text{jets}, Z \rightarrow \ell^+ \ell^-$	Charged leptons, jets
W boson	$W + \text{jets}, W \rightarrow \ell \nu$	Charged leptons, jets, prompt neutrinos
Top quark pair	$t\bar{t} \rightarrow 2\ell 2\nu 2b$	Muons, b quark jets, prompt neutrinos
<i>Higgs physics</i>		
Invisible Higgs	$qqH, H \rightarrow ZZ^* \rightarrow 4\nu$	Forward jets, prompt neutrinos
Di-Higgs	$gg \rightarrow HH \rightarrow bb\tau\tau$	τ leptons, b quark jets, prompt neutrinos
$t\bar{t}H(bb)$	$t\bar{t}H, H \rightarrow b\bar{b}$	Jets, b quark jets, charged leptons, prompt neutrinos
$t\bar{t}H(\mu\mu)$	$t\bar{t}H, H \rightarrow \mu^+ \mu^-$	Muons, jets, b quark jets, prompt neutrinos
<i>Supersymmetry</i>		
Top squark pair	$gg \rightarrow \tilde{t}\tilde{t} \rightarrow 2b4q2\tilde{\chi}_1^0$	Jets, b quark jets, dark matter candidates
Heavy neutralino	$gg \rightarrow \tilde{\chi}_2^0 \tilde{\chi}_2^0 \rightarrow ZZ\tilde{\chi}_1^0 \tilde{\chi}_1^0$	Charged leptons, jets, dark matter candidates

produced in association with a $t\bar{t}$ pair followed by the Higgs boson either decaying to a pair of b quarks or to a pair of muons and the top quarks decaying to leptons. Furthermore, two sets corresponding to the production of particles using the simplified model spectra (SMS) framework of supersymmetry are considered [30,31], both with R parity conservation and a lightest supersymmetric particle, a neutralino $\tilde{\chi}_1^0$ that acts as a dark-matter candidate. One set consists of top squark-antisquark pair production with a top squark mass of 350 GeV and a $\tilde{\chi}_1^0$ mass of 335 GeV. The final state containing two b quarks, four light quarks, and two $\tilde{\chi}_1^0$ particles [32] is selected ($t \rightarrow bq\tilde{q}\tilde{\chi}_1^0$, denoted SMS T2tt). The second set is pair production of two of the heavier neutralinos with mass 400 GeV, with each neutralino decaying into a Z boson and a $\tilde{\chi}_1^0$ with a mass of 1 GeV [33] (denoted SMS TChiZZ). Both of these processes are generated with MADGRAPH5_aMC@NLO in version 2.3.3 at LO. An overview of the simulated samples and their respective final states is given in Table I.

The simulation of the interactions of all final-state particles with the CMS detector is done with GEANT4 [34]. The simulated events are reconstructed using the same algorithms used for the data. The simulated events include pileup, with the number of additional pp interactions matching that observed in data [35,36].

V. PHYSICS OBJECT AND EVENT SELECTIONS

To select $W + \text{jets}$, $Z + \text{jets}$, and $t\bar{t}$ processes, candidate events are required to pass the isolated single-muon trigger that requires p_T above 24 GeV.

The selected muon candidates are required to satisfy a set of quality criteria based on the number of spatial measurements in the silicon tracker and the muon system, as well as the fit quality of the combined muon track [15]. Muon candidates are required to have $p_T > 25$ GeV, $|\eta| < 2.4$, and pass the so-called ‘‘tight’’ identification and isolation selections [15].

The $Z + \text{jets}$ and $t\bar{t}$ events used in the algorithm training described in Sec. VI are required to have two muons with opposite charge passing the above selections. In the studies quantifying the algorithm performance described in Sec. VII A, the dimuon invariant mass is also required to satisfy $80 < m(\mu\mu) < 100$ GeV in order to select $Z \rightarrow \mu\mu$ events and veto those with genuine \vec{p}_T^{miss} (mainly from τ leptons or electroweak decays inside the heavy-flavor jets).

The $W + \text{jets}$ simulated events and data used in Sec. VII B are required to have one muon candidate passing the muon selections.

For the studies presented in Section VII C validating the \vec{p}_T^{miss} performance in other simulated physics processes, no object or event selection is applied.

VI. THE DeepMET ALGORITHM

The DNN operates on each PF candidate individually. The candidate’s inputs include eight continuous and three categorical features:

- (1) Continuous features:
 - (a) d_{xy} , the impact parameter with respect to the LPV in the transverse plane for charged PF candidates, zero for neutral PF candidates [12];
 - (b) d_z , the impact parameter with respect to the LPV along the beam direction for charged PF candidates, zero for neutral PF candidates;
 - (c) the PUPPI weight;
 - (d) five kinematic features per particle: η , mass, p_x , p_y , and p_T ;
- (2) Categorical features:
 - (a) Particle ID: a unique integer number for the seven different types of PF candidates, i.e., electrons, muons, photons, charged hadrons, neutral hadrons, and hadronic and electromagnetic PF candidates in the HF;
 - (b) charge of the particle (-1 , 0 , or $+1$);
 - (c) an LPV association flag, referred to as the fromLPV flag. This flag indicates one of four

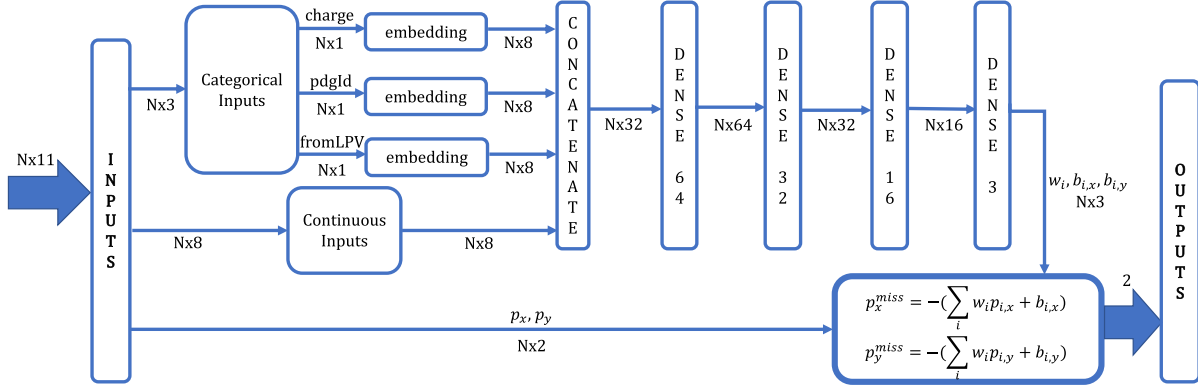


FIG. 1. DeepMET DNN architecture. For each event, all PF candidates in the event are considered as input. $N \times n$ represents the number of PF candidates in the event multiplied by the dimensionality of the per-particle feature space, where n can be 1, 2, 3, 8, 16, 32, and 64 in the architecture.

possible associations between the LPV and a charged PF candidate: used in the LPV fit; used in a pileup vertex fit; not used in any of the PV fits, but closest to one of the pileup vertices in the z direction; and not used in any of the PV fits but closest to the LPV in the z direction.

The output of the DNN is a weight (w_i) and two bias terms ($b_{i,x}, b_{i,y}$). The DeepMET estimator output is the negative of the weighted \vec{p}_T sum of all PF candidates together with their bias contributions. Its x and y components are given by,

$$\begin{aligned} p_x^{\text{miss}} &= -\sum_i (w_i p_{i,x} + b_{i,x}), \\ p_y^{\text{miss}} &= -\sum_i (w_i p_{i,y} + b_{i,y}). \end{aligned} \quad (2)$$

This calculation is similar to the PUPPI \vec{p}_T^{miss} calculation. The two bias terms in the model were initially intended to enable distinct adjustments in the x and y directions independently and to correct measurement biases. However, in practice it is found that they have minimal impact on the performance.

A. The DNN architecture

Figure 1 shows the DNN architecture. The inputs are the 11 features of each input PF candidate. After the input layer, each of the three categorical features will go through one embedding layer and become an eight-dimensional tensor, so that the feature space can be learned and the differences can be represented by distances in the embedded space.

The three eight-dimensional tensors from the embedding layers are then concatenated together with the eight continuous features, and passed to a few dense (or fully connected) layers with progressively reducing numbers of nodes. These layers act only on each particle individually and can also be considered as one-dimensional convolutions. After each dense layer, batch normalization [37] is applied (not shown in Fig. 1 for simplicity) to reduce

the covariate shifts and make the training converge faster. The outputs of these dense layers are the weights w_i , and the biases $b_{i,x}$ and $b_{i,y}$ of all the input PF candidates. In the last layer, the event \vec{p}_T^{miss} is calculated following Eq. (2).

The total number of trainable parameters in the DeepMET neural network is 4541. Such a small set of trainable parameters allows the training to converge quickly, and also significantly reduces the inference time. Studies have also been conducted using more layers and larger number of nodes per layer, and the effect on the performance was within a few percent.

The DNN architecture is implemented with KERAS [38], which acts as an interface for the TENSORFLOW [39] library. The ADAMW optimizer [40] is used for gradient optimizations.

B. Training

The DNN of DeepMET is trained with the $Z + \text{jets}$ and $t\bar{t}$ simulated samples discussed in Sec. IV. Events are required to pass the dimuon selections described in Sec. V. Using two samples allows a wide range of jet multiplicities and particle p_T distributions: $Z + \text{jets}$ events tend to have particles with low p_T ; the $t\bar{t}$ events tend to have high p_T and typically contain high- p_T neutrinos.

The \vec{p}_T^{miss} performance in $V + \text{jets}$ processes is measured by comparing the momentum of the vector boson \vec{q}_T to that of the hadronic recoil system \vec{u}_T (defined as the vector p_T sum of all PF candidates except for the decay products of the vector boson) [19]. The vector boson momenta \vec{q}_T are measured as the vector p_T sum of the two muons for Z bosons, or taken directly from the generator-level information in simulations of W bosons.

The components of the hadronic recoil parallel and perpendicular to the boson momentum vector are denoted by u_{\parallel} and u_{\perp} , respectively. These are used to study the \vec{p}_T^{miss} response and resolution. The response of \vec{p}_T^{miss} is defined as $-\langle u_{\parallel} \rangle / \langle q_T \rangle$; the resolutions of u_{\parallel} and u_{\perp} are calculated using the root-mean-square of $u_{\parallel} + q_T$ and u_{\perp}

distributions, and are denoted $\sigma(u_{\parallel})$ and $\sigma(u_{\perp})$, respectively [19].

Training is performed on an NVIDIA Quadro P6000 graphics card using a few tens of thousands of events from the $Z + \text{jets}$ sample and approximately the same number of events from the $t\bar{t}$ sample. The batch size is set to 128, and the training and validation splitting is set to 4 : 1. The training takes about 30 minutes to converge to stable results.

Further studies are performed by scanning the mixture fractions of the two samples and the hyperparameters (such as the number and size of dense layers, learning rate, training and validation splitting, and the batch size), and by increasing the number of total events in the training and validation samples. DeepMET performance is found to be only weakly sensitive to modifications of these (hyper)parameters.

C. Loss function

The loss function used in the training is the mean squared error loss,

$$L = \frac{1}{2} [(p_x^{\text{miss}} - \hat{p}_x^{\text{miss}})^2 + (p_y^{\text{miss}} - \hat{p}_y^{\text{miss}})^2] \quad (3)$$

where $p_{x,y}^{\text{miss}}$, $\hat{p}_{x,y}^{\text{miss}}$ are the predicted and generator-level components of \vec{p}_T^{miss} in the x , y directions.

VII. THE DeepMET PERFORMANCE

The DeepMET performance in data and MC simulations is discussed in this Section. Improvements in resolutions are observed, with the response closer to unity, and more pileup resilience compared with PF \vec{p}_T^{miss} and PUPPI \vec{p}_T^{miss} .

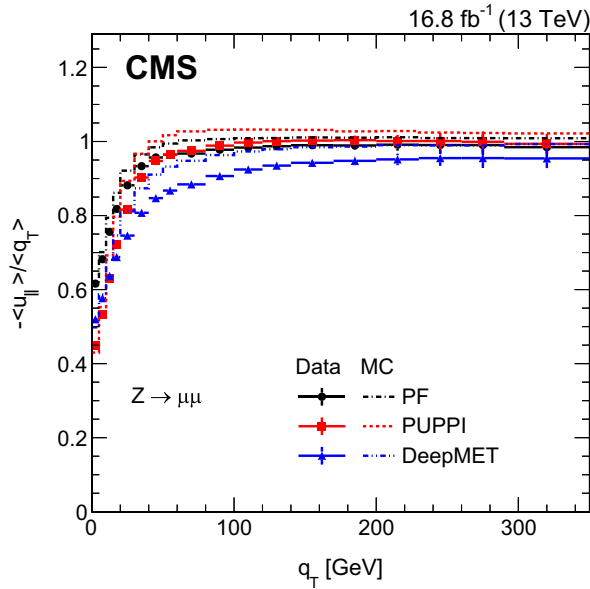


FIG. 2. Recoil responses of different \vec{p}_T^{miss} estimators in data (markers) and MC simulations (dashed) after the $Z \rightarrow \mu\mu$ selections.

The following performance studies focus primarily on the muon channel; however, comparable performance improvements were observed in the electron channel.

A. Performance on $Z + \text{jets}$ events

The \vec{p}_T^{miss} performance is studied using the events passing the $Z + \text{jets}$ selections in Sec. V. Such events should have little or no genuine \vec{p}_T^{miss} . The responses of different \vec{p}_T^{miss} estimators are shown in Fig. 2. Markers correspond to collision data, and dashed lines indicate MC simulations. The DeepMET algorithm maintains a good, albeit 5%–10% worse, response than the PF and PUPPI \vec{p}_T^{miss} estimators.

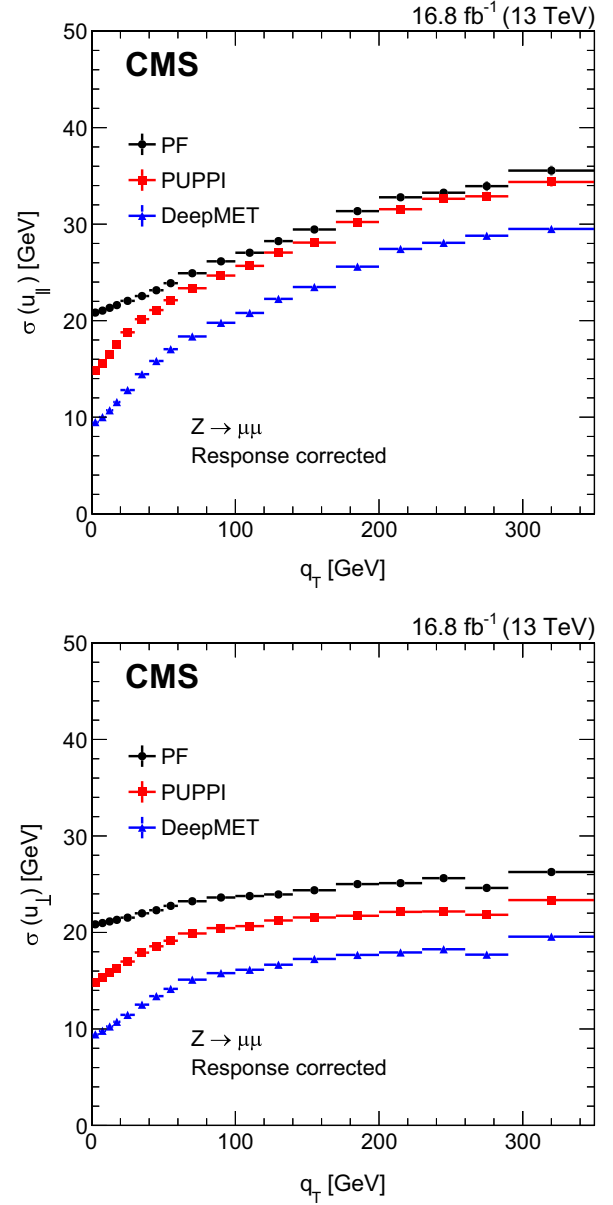


FIG. 3. Response-corrected resolutions of u_{\parallel} (upper) and u_{\perp} (lower) vs q_T of different \vec{p}_T^{miss} estimators in data after the $Z \rightarrow \mu\mu$ selections.

To properly account for the response effect on the resolutions, for each \vec{p}_T^{miss} estimator, the average response $-\langle u_{\parallel} \rangle / \langle q_T \rangle$ is calculated using the events in the response plateau region (i.e., $q_T > 150$ GeV), and the resolutions are scaled by the inverse of this average response, referred to as “response-corrected resolutions.” The response-corrected resolutions of u_{\parallel} and u_{\perp} vs q_T and the number of reconstructed PVs are shown in Figs. 3 and 4, respectively. The DeepMET algorithm maintains good resolutions and pileup resilience. Despite slightly worse response than the

PF and PUPPI \vec{p}_T^{miss} estimators, DeepMET resolutions are better even after including the response corrections. For example, compared with PUPPI \vec{p}_T^{miss} , the DeepMET shows a 2%–10% worse response but achieves a 20%–30% resolution gain around 20 reconstructed primary vertices, significantly outperforming PUPPI in this regime.

The comparisons of response-corrected resolutions of different \vec{p}_T^{miss} estimators in $Z \rightarrow \mu\mu$ events for the low- and high- q_T regions are provided in Figs. 5 and 6, respectively, corresponding to the region where $q_T < (>)50$ GeV. In both regions, PUPPI \vec{p}_T^{miss} is better than PF \vec{p}_T^{miss} , and DeepMET outperforms both \vec{p}_T^{miss} estimators.

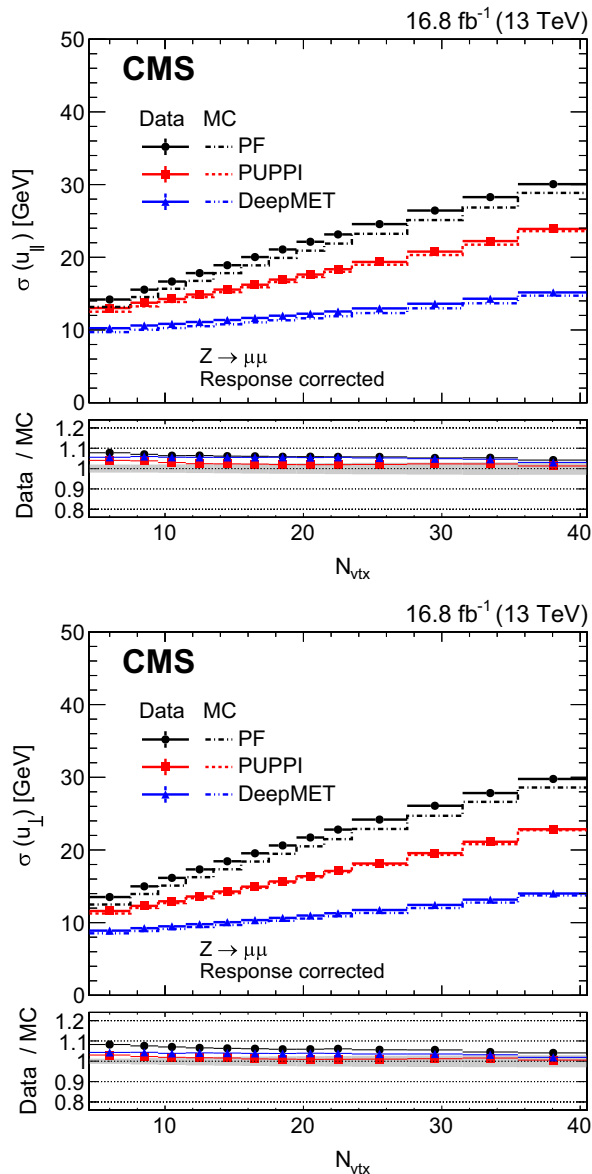


FIG. 4. Response-corrected resolutions of u_{\parallel} (upper) and u_{\perp} (lower) vs number of reconstructed PVs of different \vec{p}_T^{miss} estimators in data (solid) and MC simulations (dashed) after the $Z \rightarrow \mu\mu$ selections. The systematic uncertainties for PUPPI \vec{p}_T^{miss} due to the JES, the JER, and E_U are added in quadrature and displayed with the gray band.

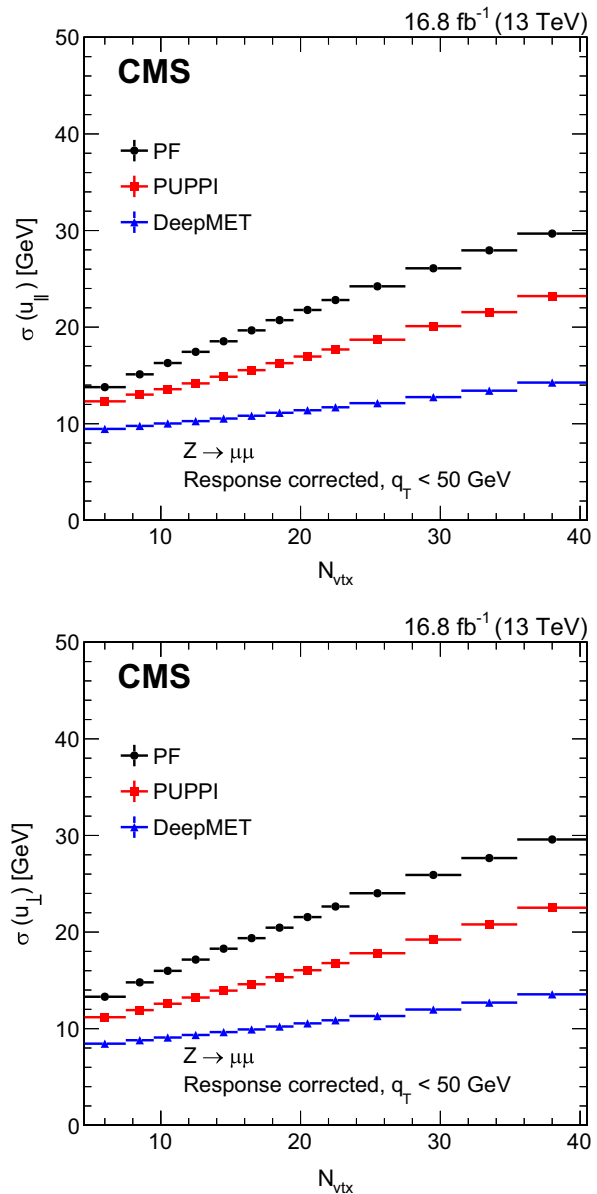


FIG. 5. Response-corrected resolutions of u_{\parallel} (upper) and u_{\perp} (lower) vs number of reconstructed PVs of different \vec{p}_T^{miss} estimators in data after the $Z \rightarrow \mu\mu$ selections in the region with q_T smaller than 50 GeV.

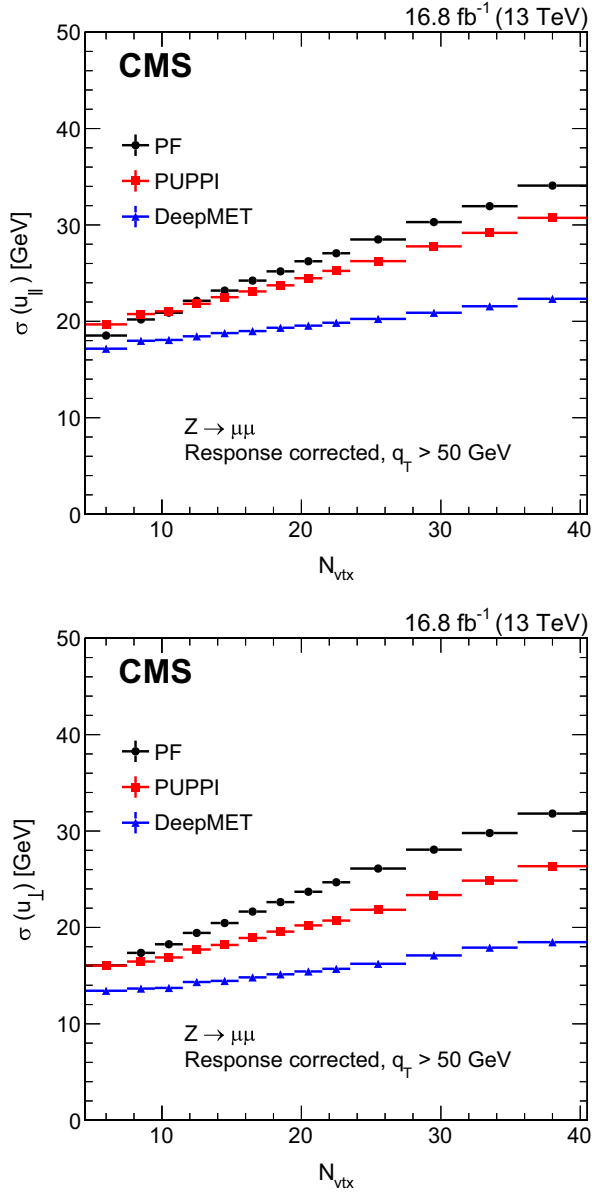


FIG. 6. Response-corrected resolutions of u_{\parallel} (upper) and u_{\perp} (lower) vs number of reconstructed PVs of different \vec{p}_T^{miss} estimators in data after the $Z \rightarrow \mu\mu$ selections in the region with q_T larger than 50 GeV.

B. The PV-Agnostic DeepMET and performance on $W + \text{jets}$ events

The performance has also been studied in $W + \text{jets}$ MC samples, in which the W boson decays into a muon and a(n) (anti)neutrino. Typically, this signal process involves a single isolated muon, genuine \vec{p}_T^{miss} , and several soft tracks as the p_T distribution of W bosons is low with the most probable value around 5 GeV [41]. In this study, the accuracy of LPV identification in approximately 1% of the events in the $W + \text{jets}$ simulations is compromised, where the LPV is either reconstructed but incorrectly identified as a pileup vertex, or is not reconstructed at all. This occurs more

frequently in events with muons at high $|\eta|$, where the quality of the muon track is worse. Such mistakes in the LPV identification can result in incorrect PV-track association flags and PUPPI weights, which in turn introduce inaccuracies in subsequent calculations of PUPPI and DeepMET \vec{p}_T^{miss} .

To handle such scenarios for high-precision $W(\mu\nu)$ analyses, a PV-agnostic version of DeepMET is developed, which is robust to the choice of the LPV from the PVs [42]. In this version of the algorithm, the default LPV selection is discarded, and instead the PV closest in z to the leading muon with $dz(\text{PV}, \mu) < 0.2$ cm is chosen. If there is no PV satisfying the requirement (i.e., the LPV is not successfully reconstructed), a “pseudo”-LPV is built, using (x, y) of the beam spot (luminous region of the pp collisions [12]), and the leading muon z position. In the DeepMET inputs, d_z 's and the PUPPI weights are recomputed with respect to the new LPV, while fromLPV and d_{xy} are not used, since they cannot be recalculated precisely. The model is retrained using the reduced set of inputs.

Figure 7 illustrates the performance comparisons of various \vec{p}_T^{miss} estimators for $W + \text{jets}$ events, with solid (dashed) lines representing events where the LPV is correctly (incorrectly) identified. As anticipated, PF \vec{p}_T^{miss} is the estimator least impacted by LPV identification issues. Conversely, both PUPPI \vec{p}_T^{miss} and the original DeepMET are significantly influenced. The PV-Agnostic approach helps to mitigate the dependence on LPV identifications, resulting in comparable performance between events with correct and incorrect LPV assignment. The remaining discrepancy is similar to that of PF \vec{p}_T^{miss} , which is primarily due to different kinematic distributions (e.g., larger fraction of LPV-incorrect events for those with muons at higher $|\eta|$).

The \vec{p}_T^{miss} and W boson transverse mass [defined as $m_T = \sqrt{2p_T^\mu p_T^{\text{miss}} [1 - \cos(\Delta\phi)]}$, where $\Delta\phi$ is the azimuthal angle difference between muon p_T and \vec{p}_T^{miss}] distributions are shown in Fig. 8 for data after the $W \rightarrow \mu\nu$ selections. Table II gives a \vec{p}_T^{miss} resolution metric: the higher half width at half maximum, defined as the difference between the value of $p_T^{\text{miss}}(m_T)$ at the $p_T^{\text{miss}}(m_T)$ probability density function (pdf) distribution maximum and the larger of the two values whose pdf is half the maximum value. For both variables, DeepMET (PV-Agnostic) has a sharper Jacobian peak and thus provides better resolution.

C. Performance for other physics processes

The \vec{p}_T^{miss} resolution of different estimators is also compared for a number of physics processes with genuine \vec{p}_T^{miss} . The samples are listed in Sec. IV, and are used without any specific event selection applied. Figure 9 shows the p_T^{miss} resolution for the DeepMET, PUPPI \vec{p}_T^{miss} , and PF \vec{p}_T^{miss} algorithms as a function of the sum of the p_T 's of generated jets (H_T) for various physics processes for which p_T^{miss} is expected to have a crucial role in the event selection and/or reconstruction, and hence for the final physics sensitivity.

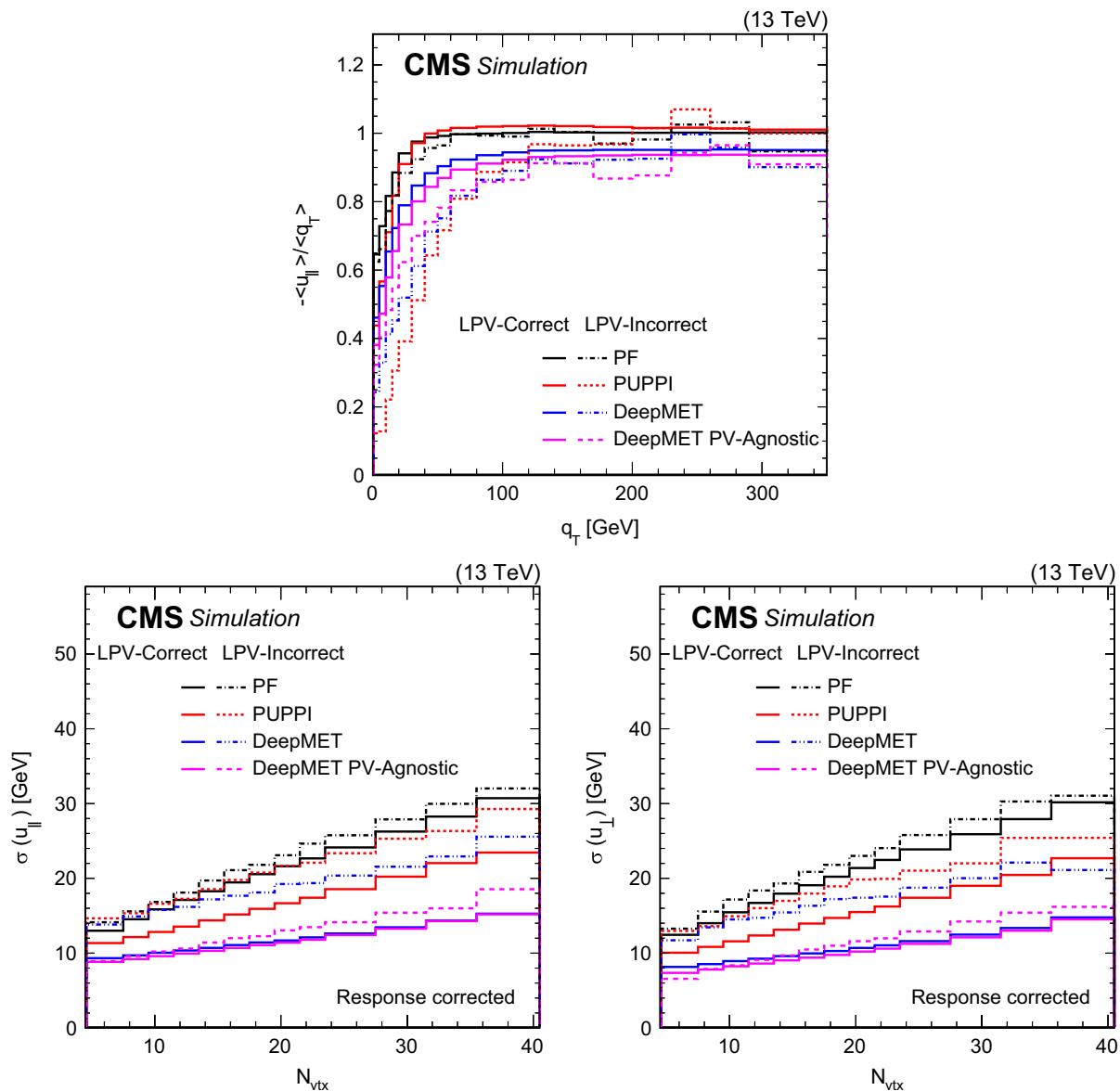


FIG. 7. Response (upper), response-corrected resolutions of u_{\parallel} (lower left) and u_{\perp} (lower right) of different \vec{p}_T^{miss} estimators in $W + \text{jets}$ MC simulations. Solid (dashed) lines are from events where the LPV is (in)correctly identified.

DeepMET demonstrates superior resolution in p_T^{miss} for all considered physics processes, including Higgs boson production with decays to SM particles, Higgs boson decay to dark matter candidates, and the supersymmetric processes described in Sec. IV. These processes include a wide range of different jet and lepton multiplicities and jet flavors, and cover a broad kinematic range. The relative improvement in resolution is largest for low values of generator jet H_T , i.e., for low amounts of hard hadronic activity, indicating that DeepMET particularly helps with the softer contributions to \vec{p}_T^{miss} .

VIII. THE DeepMET CALIBRATIONS

The DeepMET calibrations can be derived from $Z + \text{jets}$ events by matching the performance in MC simulations to data. These corrections can be applied to the DNN outputs.

Since the calibrations are only applied to MC simulations, all the performance results on data shown in the previous Sections are unchanged after calibration.

A. The XY correction

Due to asymmetries in the detector responses and resolutions, and also because of the offset of the beam spot position, etc., the reconstructed \vec{p}_T^{miss} response depends on ϕ . The average values of \vec{p}_T^{miss} in the x and y directions are calculated as a function of the number of PVs and then subtracted from the individual \vec{p}_T^{miss} components, centering the distributions at zero. The ϕ distributions of different \vec{p}_T^{miss} estimators before and after the xy correction are shown in Fig. 10. The distribution becomes flat, as expected, for both data and MC simulations after correction.

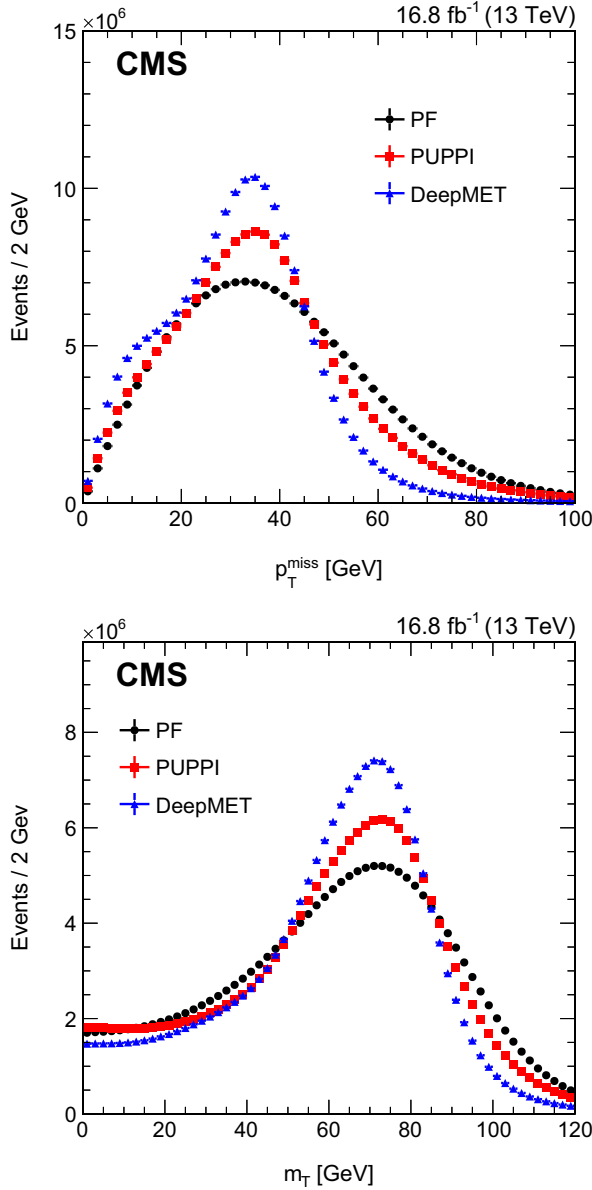


FIG. 8. Distributions of p_T^{miss} (left) and m_T (right) of different \vec{p}_T^{miss} estimators in data after $W \rightarrow \mu\nu$ selections.

B. Scale and resolution calibration

Since the jet and PF candidate resolutions are typically worse in data than predicted from simulation, a quantile-based calibration is performed. The calibration is done in four main steps.

TABLE II. Higher half width at half maximum in p_T^{miss} and m_T in data after the $W \rightarrow \mu\nu$ selections.

Higher half width at half maximum/GeV	p_T^{miss}	m_T
PF	25.4	27.0
PUPPI	18.4	16.2
DeepMET (PV-agnostic)	15.2	13.0

First the data and MC simulations are binned in q_T of the Z boson. For the data, the contributions from $t\bar{t}$ and diboson production are estimated from MC simulation and subtracted. Each bin's u_{\parallel} and u_{\perp} distribution is fitted with a double-Gaussian function.

In the second step, each of the fitted double-Gaussian functions is integrated to get the corresponding cumulative distribution functions (CDFs).

In MC simulation, the u_{\parallel} and u_{\perp} CDF values in the i th q_T bin can be found from,

$$\begin{aligned} p_{\parallel} &= \text{CDF}_i^{u_{\parallel}, \text{MC}}(u_{\parallel}^{\text{MC}}), \\ p_{\perp} &= \text{CDF}_i^{u_{\perp}, \text{MC}}(u_{\perp}^{\text{MC}}). \end{aligned} \quad (4)$$

In data, the corresponding u_{\parallel} and u_{\perp} CDF in the same q_T bin is given by,

$$\begin{aligned} u_{\parallel}^{\text{data}} &= (\text{CDF}_i^{u_{\parallel}, \text{data}})^{-1}(p_{\parallel}), \\ u_{\perp}^{\text{data}} &= (\text{CDF}_i^{u_{\perp}, \text{data}})^{-1}(p_{\perp}). \end{aligned} \quad (5)$$

Finally the differences $u_{\parallel}^{\text{data}} - u_{\parallel}^{\text{MC}}$ and $u_{\perp}^{\text{data}} - u_{\perp}^{\text{MC}}$ are applied as the corrections to u_{\parallel} and u_{\perp} in simulation, respectively. The corrected DeepMET is then calculated from the corrected u_{\parallel} and u_{\perp} .

C. Data vs simulation comparisons after calibration

Figure 11 illustrates the data-simulation comparisons for DeepMET p_T^{miss} (upper left), recoil p_T (upper right), u_{\parallel} (lower left), and u_{\perp} (lower right) in $Z + \text{jets}$ events, after applying the calibrations. A Z boson p_T reweighting is applied to align the boson p_T distribution between data and simulation. Good agreement between data and simulation after the calibrations is observed within the systematic uncertainties, which are detailed in Sec. VIII D.

D. Systematic uncertainties from calibration

The systematic uncertainties affecting DeepMET are estimated during the calibration process. Three main sources are considered:

- (i) Jet multiplicity binning: in the default setup, the Z boson p_T is used to derive corrections in different bins. One alternative choice is to have bins in both the p_T of the Z boson and CHS jet multiplicity. A new set of corrections are derived using the same setup but with two-dimensional binning, and the difference between using both the p_T of the Z boson and the jet multiplicity, and using only the p_T of the Z boson, is chosen as one systematic uncertainty.
- (ii) Choice of the modeling function: in the default setup, a double-Gaussian function is chosen to model the u_{\parallel} and u_{\perp} distributions. To estimate the possible bias due to this choice, a Gaussian smoothing function is

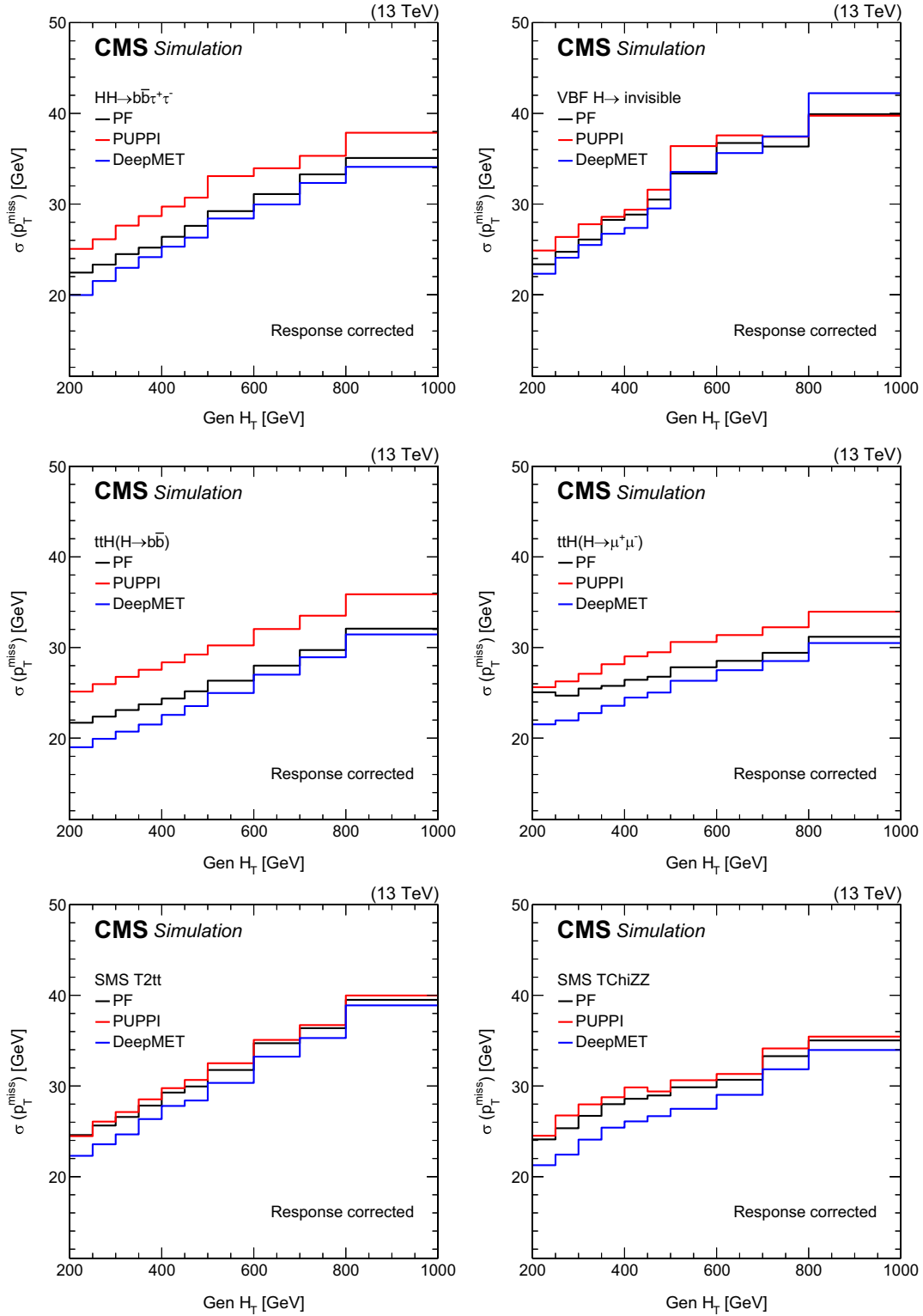


FIG. 9. Comparison of p_T^{miss} resolution for various physics processes in simulated events. The considered processes are HH production via gluon fusion with $HH \rightarrow b\bar{b}\tau\tau$ (upper left), H production via vector boson fusion with $H \rightarrow \text{invisible}$ (upper right), ttH production with $t\bar{t}$, where both top quarks decay to leptons and either $H \rightarrow b\bar{b}$ (middle left) or $H \rightarrow \mu\mu$ (middle right), the SMS T2tt process (lower left), and the SMS TChiZZ process (lower right).

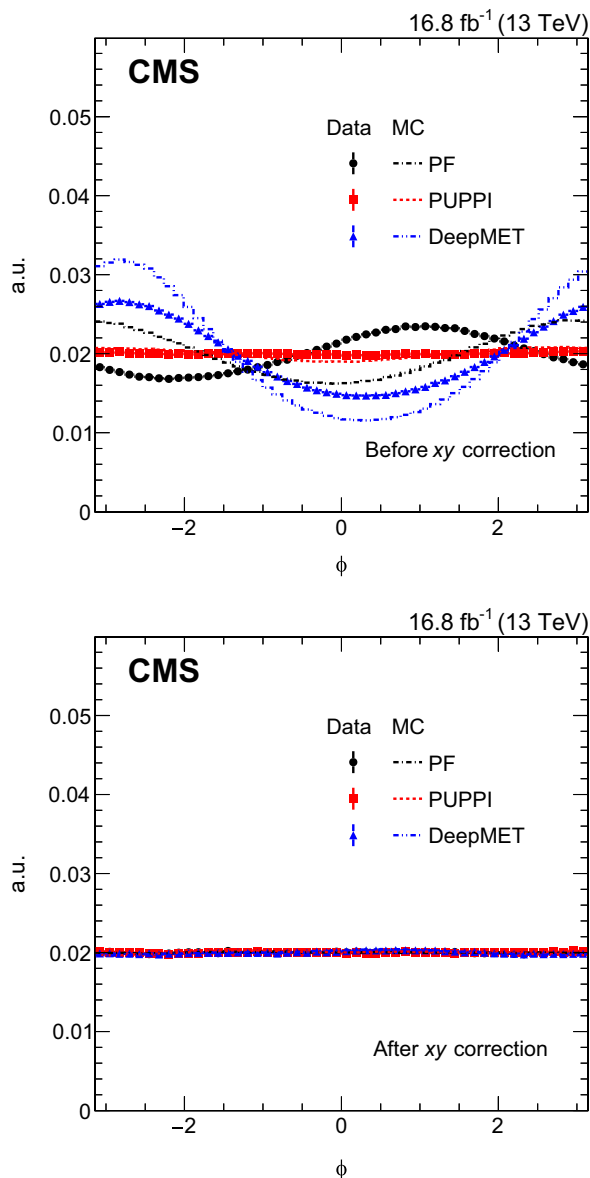


FIG. 10. ϕ distribution of different \vec{p}_T^{miss} estimators before (upper) and after (lower) the xy corrections, in data (markers) and MC simulations (dashed) after the $Z \rightarrow \mu\mu$ selections.

used to smooth the u_{\parallel} and u_{\perp} distributions, and then the CDFs and corrections are derived using the smoothed distributions. The correction difference between the double-Gaussian and Gaussian smoothing functions is chosen as one systematic uncertainty.

- (iii) Background estimation and subtraction. When fitting the data distributions, the background contributions from $t\bar{t}$ and diboson processes are estimated using MC simulation and then subtracted from data. To estimate the systematic uncertainties from the background subtraction, the contributions estimated from background MC samples are varied by $\pm 10\%$ (typical cross section measurement and theoretical uncertainties), and the difference between the calibrations

using the central values and using these are taken as the systematic uncertainty.

The total uncertainties are shown in the gray band of Fig. 11. Around the peak of the $Z + \text{jets}$ distributions (low p_T^{miss} and smaller $|u_{\perp}|$), the relative difference is around a few percent. In the tail regions the uncertainty can be as large as 10%–15%. Similar studies have also been carried out in the $t\bar{t}$ region by selecting two muons and one b jet, where good data-to-simulation agreement has also been observed after applying the corrections.

IX. TRAINING WITHOUT PUPPI WEIGHTS

To understand the role and the importance of the PUPPI weights in DeepMET’s performance, a version of DeepMET is trained without the PUPPI weight information. Because of the DNN nature of the architecture, particle-level information is not shared between different PF candidates, and the PUPPI weight is the *only* input that contains local neighborhood information. This comparison sheds light on the relative importance of a particle’s neighborhood in the observed performance improvement.

Figure 12 shows comparisons of the response and response-corrected resolution of DeepMET trained with (blue) and without (green) PUPPI weights, along with PF \vec{p}_T^{miss} and PUPPI \vec{p}_T^{miss} , after $Z \rightarrow \mu\mu$ selections. As can be seen for the $Z \rightarrow \mu\mu$ physics process, PUPPI weights mostly contribute to response improvements; the resolutions with and without PUPPI weights are similar.

X. COMPUTATIONAL PERFORMANCE

The model trained using KERAS is stored as a frozen graph in TENSORFLOW format and integrated into the CMS software framework CMSSW for subsequent inference processes. The CMSSW framework is an open-source software framework utilized in triggering, data reconstruction, simulation, and offline analysis [43,44]. In this setup, the number of input PF candidates is set to 4500, determined as the maximum count of PF candidates under the current operational conditions (typically ranging from 1500 to 2000). The model inputs consist of the 11 features of each PF candidate, as discussed in Sec. VI. In cases where there are fewer PF candidates, the input features are padded with zeros. The model processes these inputs to compute \vec{p}_T^{miss} in the x and y directions as the outputs. DeepMET inference can be performed at any stage of data processing, as long as the list of PF candidates is provided.

The computational time is also examined. When running with one thread on a single CPU core, the average processing time for the DeepMET inference within CMSSW is approximately 10 ms [45], while the total event processing time ranges from 1 to 10s, depending on the event complexity and the associated data tier. Due to the compact size of the model, the average processing time for DeepMET is much shorter than the overall CMSSW processing time.

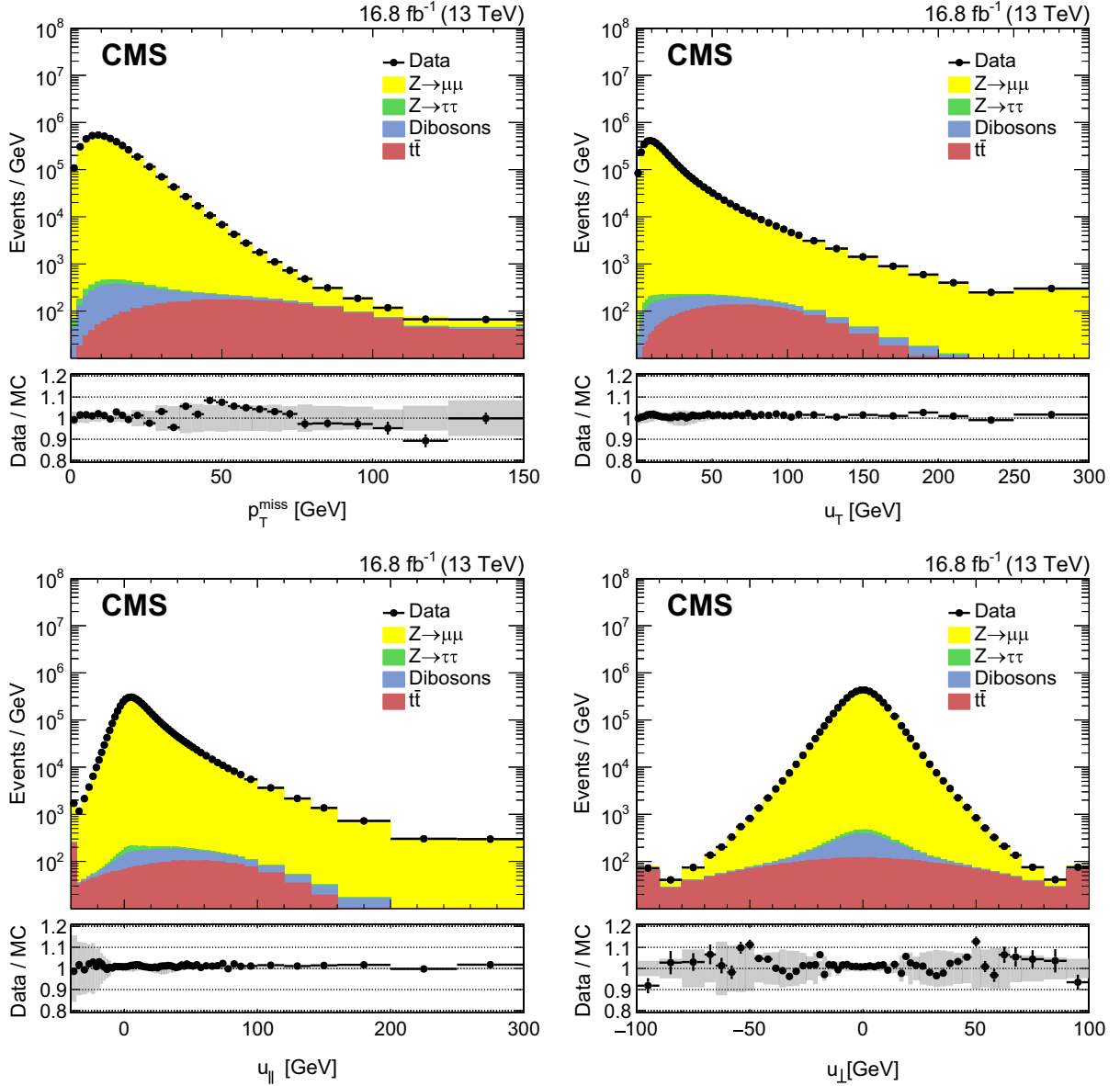


FIG. 11. Data-to-simulation comparisons of DeepMET p_T^{miss} (upper left), recoil p_T (upper right), u_{\parallel} (lower left), and u_{\perp} (lower right) after the quantile correction. The underflow (overflow) contents are included in the first (last) bin. The gray band represents the systematic uncertainties discussed in Sec. VIII D.

XI. SUMMARY

This paper presents a new \vec{p}_T^{miss} estimator, DeepMET, which is based on a deep neural network. The DeepMET algorithm utilizes each individual particle reconstructed by the CMS particle-flow algorithm as input and assigns a weight w_i and two bias terms, $b_{i,x}$ and $b_{i,y}$, to each candidate. The estimated \vec{p}_T^{miss} is the negative vector sum of the weighted transverse momenta of all candidates, plus their bias contributions.

With 4541 trainable parameters, the training and deployment of DeepMET is computationally efficient. DeepMET is trained using $Z + \text{jets}$ and $t\bar{t}$ samples, but achieves 10%–30% better resolution compared with the current

PF and PUPPI \vec{p}_T^{miss} estimators across multiple physics processes, such as $Z + \text{jets}$, $W + \text{jets}$, Higgs boson production, and processes with dark matter candidates. Another important feature of the DeepMET algorithm is its high resilience to pileup, improving the physics reach in LHC Run 2 and Run 3, and future high-luminosity LHC conditions. Specifically for the measurement of the W boson mass, a PV-agnostic version of DeepMET is designed to be more robust in $W \rightarrow \mu\nu$ events where the LPV is not always identified correctly. Events containing $Z \rightarrow \mu\mu$ decays are used to calibrate \vec{p}_T^{miss} , including corrections for asymmetries in detector response, as well as for \vec{p}_T^{miss} scale and resolution.

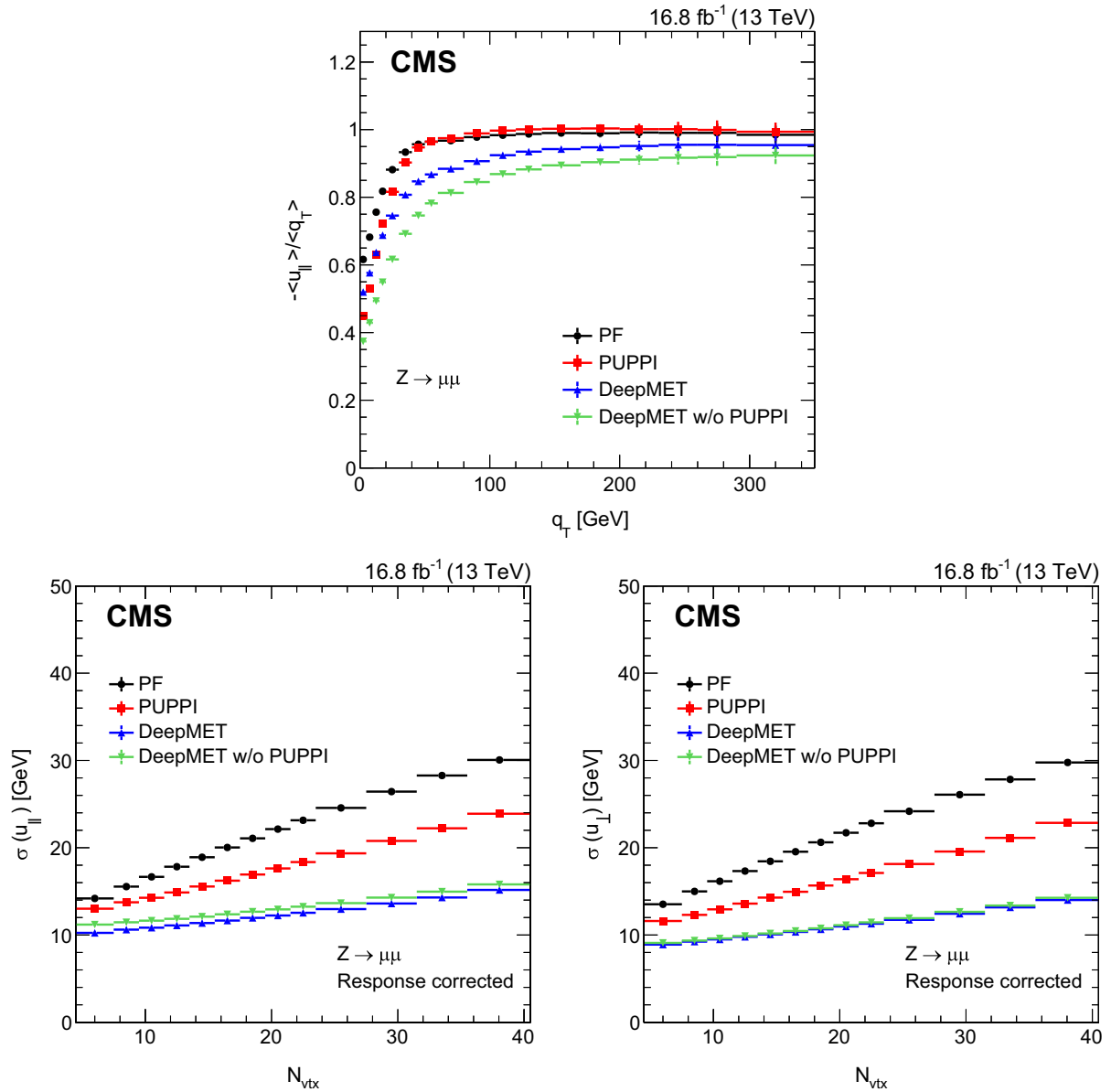


FIG. 12. Response (upper) and response-corrected resolutions of u_{\parallel} (lower left) and u_{\perp} (lower right) of different $\vec{p}_{\text{T}}^{\text{miss}}$ estimators in data after the $Z \rightarrow \mu\mu$ selections.

Good agreement between data and simulation is found. The DeepMET estimator demonstrates the potential to improve the precision of SM measurements and to achieve higher sensitivity in beyond the standard model physics searches.

ACKNOWLEDGMENTS

We congratulate our colleagues in the CERN accelerator departments for the excellent performance of the LHC and thank the technical and administrative staffs at CERN and at other CMS institutes for their contributions to the success of the CMS effort. In addition, we gratefully acknowledge the computing centers and personnel of the Worldwide LHC

Computing Grid and other centers for delivering so effectively the computing infrastructure essential to our analyses. Finally, we acknowledge the enduring support for the construction and operation of the LHC, the CMS detector, and the supporting computing infrastructure provided by the following funding agencies: SC (Armenia), BMBWF and FWF (Austria); FNRS and FWO (Belgium); CNPq, CAPES, FAPERJ, FAPERGS, and FAPESP (Brazil); MES and BNSF (Bulgaria); CERN; CAS, MoST, and NSFC (China); Minciencias (Colombia); MSES and CSF (Croatia); RIF (Cyprus); SENESCYT (Ecuador); ERC PRG, TARISTU24-TK10 and MoER TK202 (Estonia); Academy of Finland, MEC, and HIP (Finland); CEA and CNRS/IN2P3 (France); SRNSF (Georgia); BMFTR, DFG,

and HGF (Germany); GSRI (Greece); NKFIH (Hungary); DAE and DST (India); IPM (Iran); SFI (Ireland); INFN (Italy); MSIT and NRF (Republic of Korea); MES (Latvia); LMTLT (Lithuania); MOE and UM (Malaysia); BUAP, CINVESTAV, CONACYT, LNS, SEP, and UASLP-FAI (Mexico); MOS (Montenegro); MBIE (New Zealand); PAEC (Pakistan); MES, NSC, and NAWA (Poland); FCT (Portugal); MESTD (Serbia); MICIU/AEI and PCTI (Spain); MOSTR (Sri Lanka); Swiss Funding Agencies (Switzerland); MST (Taipei); MHESI and NSTDA (Thailand); TUBITAK and TENMAK (Türkiye); NASU (Ukraine); STFC (United Kingdom); DOE and NSF (USA). Individuals have received support from the Marie-Curie program and the European Research Council and Horizon 2020 Grant, Contracts No. 675440, No. 724704, No. 752730, No. 758316, No. 765710, No. 824093, No. 101115353, No. 101002207, No. 101001205, and COST Action CA16108 (European Union); the Leventis Foundation; the Alfred P. Sloan Foundation; the Alexander von Humboldt Foundation; the Science Committee, Project No. 22r1-037 (Armenia); the Fonds pour la Formation à la Recherche dans l'Industrie et dans l'Agriculture (FRIA-Belgium); the Beijing Municipal Science & Technology Commission, Grant No. Z191100007219010, the Fundamental Research Funds for the Central Universities, the Ministry of Science and Technology of China under Grant No. 2023YFA1605804, and the Natural Science Foundation of China under Grant No. 12061141002 (China); the Ministry of Education, Youth and Sports (MEYS) of the Czech Republic; the Shota Rustaveli National Science Foundation, Grant No. FR-22-985 (Georgia); the Deutsche Forschungsgemeinschaft (DFG), among others, under Germany's Excellence Strategy—EXC 2121 “Quantum Universe”—390833306, and under Project No. 400140256—GRK2497; the Hellenic Foundation for Research and Innovation (HFRI), Project No. 2288 (Greece); the Hungarian Academy of Sciences, the New

National Excellence Program—ÚNKP, the NKFIH research Grants No. K 131991, No. K 133046, K 138136, No. K 143460, No. K 143477, No. K 146913, No. K 146914, No. K 147048, No. 2020-2.2.1-ED-2021-00181, No. TKP2021-NKTA-64, and No. 2021-4.1.2-NEMZ_KI-2024-00036 (Hungary); the Council of Science and Industrial Research, India; ICSC—National Research Center for High Performance Computing, Big Data and Quantum Computing, FAIR—Future Artificial Intelligence Research, and CUP I53D23001070006 (Mission 4 Component 1), funded by the NextGenerationEU program (Italy); the Latvian Council of Science; the Ministry of Education and Science, Project No. 2022/WK/14, and the National Science Center, Contracts Opus No. 2021/41/B/ST2/01369, No. 2021/43/B/ST2/01552, No. 2023/49/B/ST2/03273, and the NAWA Contract No. BPN/PPO/2021/1/00011 (Poland); the Fundação para a Ciência e a Tecnologia, Grant No. CEECIND/01334/2018 (Portugal); the National Priorities Research Program by Qatar National Research Fund; MICIU/AEI/10.13039/501100011033, ERDF/EU, “European Union NextGenerationEU/PRTR,” and Programa Severo Ochoa del Principado de Asturias (Spain); the Chulalongkorn Academic into Its 2nd Century Project Advancement Project, and the National Science, Research and Innovation Fund via the Program Management Unit for Human Resources & Institutional Development, Research and Innovation, Grant No. B39G680009 (Thailand); the Kavli Foundation; the Nvidia Corporation; the SuperMicro Corporation; the Welch Foundation, Contract No. C-1845; and the Weston Havens Foundation (USA).

DATA AVAILABILITY

Release and preservation of data used by the CMS Collaboration as the basis for publications is guided by the CMS data preservation, reuse and open access policy [46].

-
- [1] CMS Collaboration, The CMS experiment at the CERN LHC, *J. Instrum.* **3**, S08004 (2008).
 - [2] ATLAS Collaboration, The ATLAS experiment at the CERN Large Hadron Collider, *J. Instrum.* **3**, S08003 (2008).
 - [3] CMS Collaboration, Pileup mitigation at CMS in 13 TeV data, *J. Instrum.* **15**, P09018 (2020).
 - [4] D. Bertolini, P. Harris, M. Low, and N. Tran, Pileup per particle identification, *J. High Energy Phys.* **10** (2014) 059.
 - [5] CMS Collaboration, Pileup-per-particle identification: Optimisation for Run 2 Legacy and beyond, CMS detector performance summary, Report No. CMS-DP-2021-001, 2021, <https://cds.cern.ch/record/2751563>.
 - [6] CMS Collaboration, Performance of the CMS missing transverse momentum reconstruction in pp data at $\sqrt{s} = 8$ TeV, *J. Instrum.* **10**, P02006 (2014).
 - [7] CMS Collaboration, Evidence for the 125 GeV Higgs boson decaying to a pair of τ leptons, *J. High Energy Phys.* **05** (2014) 104.
 - [8] HEPData record for this analysis (2025), [10.17182/hepdata.159179](https://hepdata.cern.ch/record/159179).
 - [9] CMS Collaboration, Performance of the CMS Level-1 trigger in proton-proton collisions at $\sqrt{s} = 13$ TeV, *J. Instrum.* **15**, P10017 (2020).
 - [10] CMS Collaboration, The CMS trigger system, *J. Instrum.* **12**, P01020 (2016).

- [11] CMS Collaboration, Performance of the CMS high-level trigger during LHC Run 2, *J. Instrum.* **19**, P11021 (2024).
- [12] CMS Collaboration, Description and performance of track and primary-vertex reconstruction with the CMS tracker, *J. Instrum.* **9**, P10009 (2014).
- [13] CMS Collaboration, Technical proposal for the Phase-II upgrade of the compact muon solenoid, CMS technical proposal, Report Nos. CERN-LHCC-2015-010, CMS-TDR-15-02, 2015, <http://cds.cern.ch/record/2020886>.
- [14] CMS Collaboration, Particle-flow reconstruction and global event description with the CMS detector, *J. Instrum.* **12**, P10003 (2017).
- [15] CMS Collaboration, Performance of the CMS muon detector and muon reconstruction with proton-proton collisions at $\sqrt{s} = 13$ TeV, *J. Instrum.* **13**, P06015 (2018).
- [16] M. Cacciari, G. P. Salam, and G. Soyez, The anti- k_T jet clustering algorithm, *J. High Energy Phys.* **04** (2008) 063.
- [17] M. Cacciari, G. P. Salam, and G. Soyez, FastJet user manual, *Eur. Phys. J. C* **72**, 1896 (2012).
- [18] CMS Collaboration, Jet energy scale and resolution in the CMS experiment in pp collisions at 8 TeV, *J. Instrum.* **12**, P02014 (2016).
- [19] CMS Collaboration, Performance of missing transverse momentum reconstruction in proton-proton collisions at $\sqrt{s} = 13$ TeV using the CMS detector, *J. Instrum.* **14**, P07004 (2019).
- [20] CMS Collaboration, Precision luminosity measurement in proton-proton collisions at $\sqrt{s} = 13$ TeV in 2015 and 2016 at CMS, *Eur. Phys. J. C* **81**, 800 (2021).
- [21] J. Alwall, R. Frederix, S. Frixione, V. Hirschi, F. Maltoni, O. Mattelaer, H. S. Shao, T. Stelzer, P. Torrielli, and M. Zaro, The automated computation of tree-level and next-to-leading order differential cross sections, and their matching to parton shower simulations, *J. High Energy Phys.* **07** (2014) 079.
- [22] P. Nason, A new method for combining NLO QCD with shower Monte Carlo algorithms, *J. High Energy Phys.* **11** (2004) 040.
- [23] S. Frixione, P. Nason, and C. Oleari, Matching NLO QCD computations with parton shower simulations: The POWHEG method, *J. High Energy Phys.* **11** (2007) 070.
- [24] S. Alioli, P. Nason, C. Oleari, and E. Re, NLO vector-boson production matched with shower in POWHEG, *J. High Energy Phys.* **07** (2008) 060.
- [25] S. Alioli, P. Nason, C. Oleari, and E. Re, A general framework for implementing NLO calculations in shower Monte Carlo programs: the POWHEG BOX, *J. High Energy Phys.* **06** (2010) 043.
- [26] T. Sjöstrand, S. Ask, J. R. Christiansen, R. Corke, N. Desai, P. Ilten, S. Mrenna, S. Prestel, C. O. Rasmussen, and P. Z. Skands, An introduction to PYTHIA8.2, *Comput. Phys. Commun.* **191**, 159 (2015).
- [27] P. Skands, S. Carrazza, and J. Rojo, Tuning PYTHIA8.1: The Monash 2013 tune, *Eur. Phys. J. C* **74**, 3024 (2014).
- [28] CMS Collaboration, Extraction and validation of a new set of CMS PYTHIA8 tunes from underlying-event measurements, *Eur. Phys. J. C* **80**, 4 (2020).
- [29] R. D. Ball *et al.* (NNPDF Collaboration), Parton distributions from high-precision collider data, *Eur. Phys. J. C* **77**, 663 (2017).
- [30] J. Alwall, P. C. Schuster, and N. Toro, Simplified models for a first characterization of new physics at the LHC, *Phys. Rev. D* **79**, 075020 (2009).
- [31] LHC New Physics Working Group, Simplified models for LHC new physics searches, *J. Phys. G* **39**, 105005 (2012).
- [32] CMS Collaboration, Search for supersymmetry in proton-proton collisions at 13 TeV in final states with jets and missing transverse momentum, *J. High Energy Phys.* **10** (2019) 244.
- [33] CMS Collaboration, Search for electroweak production of charginos and neutralinos at $\sqrt{s} = 13$ TeV in final states containing hadronic decays of WW, WZ, or WH and missing transverse momentum, *Phys. Lett. B* **842**, 137460 (2023).
- [34] S. Agostinelli *et al.* (GEANT4 Collaboration), GEANT4—A simulation toolkit, *Nucl. Instrum. Methods Phys. Res., Sect. A* **506**, 250 (2003).
- [35] CMS Collaboration, Upgrades for the CMS simulation, *J. Phys. Conf. Ser.* **608**, 012056 (2015).
- [36] CMS Collaboration, Measurement of the inelastic proton-proton cross section at $\sqrt{s} = 13$ TeV, *J. High Energy Phys.* **07** (2018) 161.
- [37] S. Ioffe and C. Szegedy, Batch normalization: accelerating deep network training by reducing internal covariate shift, [arXiv:1502.03167](https://arxiv.org/abs/1502.03167).
- [38] F. Chollet *et al.*, Keras, <https://keras.io> (2015).
- [39] M. Abadi *et al.*, TensorFlow: A system for large-scale machine learning, [arXiv:1605.08695](https://arxiv.org/abs/1605.08695).
- [40] I. Loshchilov and F. Hutter, Decoupled weight decay regularization, [arXiv:1711.05101](https://arxiv.org/abs/1711.05101).
- [41] CMS Collaboration, Measurement of the transverse momentum spectra of weak vector bosons produced in proton-proton collisions at $\sqrt{s} = 8$ TeV, *J. High Energy Phys.* **02** (2017) 096.
- [42] CMS Collaboration, High-precision measurement of the W boson mass with the CMS experiment at the LHC, [arXiv:2412.13872](https://arxiv.org/abs/2412.13872).
- [43] CMS Collaboration, CMS physics: Technical design report Volume 1: Detector performance and software, CMS Technical Design Report, Report Nos. CERN-LHCC-2006-001, CMS-TDR-8-1, 2006, <https://cds.cern.ch/record/922757>.
- [44] CMS Collaboration, CMSSW on Github, accessed: 2023-11-08, <http://cms-sw.github.io/>.
- [45] CMS Collaboration, Portable acceleration of CMS computing workflows with coprocessors as a service, *Comput. Software Big Sci.* **8**, 17 (2024).
- [46] CMS Collaboration, 2020 CMS data preservation, re-use and open access policy. CERN Open Data Portal (2020), [10.7483/OPENDATA.CMS.1BNU.8V1W](https://cds.cern.ch/record/2748337).

A. Hayrapetyan,¹ V. Makarenko¹ , A. Tumasyan¹ ,^{1,b} W. Adam² , J. W. Andrejkovic,² L. Benato² , T. Bergauer² , M. Dragicevic² , C. Giordano,² P. S. Hussain² , M. Jeitler^{2,c} , N. Krammer² , A. Li² , D. Liko² , M. Matthewman,² I. Mikulec² , J. Schieck^{2,c} , R. Schöfbeck^{2,c} , D. Schwarz² , M. Shooshitari,² M. Sonawane² , W. Waltenberger² , C.-E. Wulz^{2,c} , T. Janssen³ , H. Kwon³ , D. Ocampo Henao³ , T. Van Laer³ , P. Van Mechelen³ , J. Bierkens³ , N. Breugelmans,⁴ J. D'Hondt⁴ , S. Dansana⁴ , A. De Moor⁴ , M. Delcourt⁴ , F. Heyen,⁴ Y. Hong⁴ , P. Kashko⁴ , S. Lowette⁴ , I. Makarenko⁴ , D. Müller⁴ , J. Song⁴ , S. Tavernier⁴ , M. Tytgat^{4,d} , G. P. Van Onsem⁴ , S. Van Putte⁴ , D. Vannerom⁴ , B. Bilin⁵ , B. Clerbaux⁵ , A. K. Das,⁵ I. De Bruyn⁵ , G. De Lentdecker⁵ , H. Evard⁵ , L. Favart⁵ , P. Gianneios⁵ , A. Khalilzadeh,⁵ F. A. Khan⁵ , A. Malara⁵ , M. A. Shahzad,⁵ L. Thomas⁵ , M. Vanden Bemden⁵ , C. Vander Velde⁵ , P. Vanlaer⁵ , F. Zhang⁵ , M. De Coen⁶ , D. Dobur⁶ , G. Gokbulut⁶ , J. Knolle⁶ , D. Marckx⁶ , K. Skovpen⁶ , A. M. Tomaru,⁶ N. Van Den Bossche⁶ , J. van der Linden⁶ , J. Vandenbroeck⁶ , L. Wezenbeek⁶ , S. Bein⁷ , A. Benecke⁷ , A. Bethani⁷ , G. Bruno⁷ , A. Cappati⁷ , J. De Favereau De Jeneret⁷ , C. Delaere⁷ , A. Giammanco⁷ , A. O. Guzel⁷ , V. Lemaitre,⁷ J. Lidrych⁷ , P. Malek⁷ , P. Mastrapasqua⁷ , S. Turcpar⁷ , G. A. Alves⁸ , M. Barroso Ferreira Filho⁸ , E. Coelho⁸ , C. Hensel⁸ , T. Menezes De Oliveira⁸ , C. Mora Herrera^{8,e} , P. Rebello Teles⁸ , M. Soeiro⁸ , E. J. Tonelli Manganote^{8,f} , A. Vilela Pereira^{8,e} , W. L. Aldá Júnior⁹ , H. Brandao Malbouisson⁹ , W. Carvalho⁹ , J. Chinellato^{9,g} , M. Costa Reis⁹ , E. M. Da Costa⁹ , G. G. Da Silveira^{9,h} , D. De Jesus Damiao⁹ , S. Fonseca De Souza⁹ , R. Gomes De Souza⁹ , S. S. Jesus⁹ , T. Laux Kuhn⁹ ,^{9,h} M. Macedo⁹ , K. Mota Amarilo⁹ , L. Mundim⁹ , H. Nogima⁹ , J. P. Pinheiro⁹ , A. Santoro⁹ , A. Sznajder⁹ , M. Thiel⁹ , F. Torres Da Silva De Araujo^{9,i} , C. A. Bernardes⁹ ,^{10,h} F. Damas¹⁰ , T. R. Fernandez Perez Tomei,¹⁰ E. M. Gregores¹⁰ , B. Lopes Da Costa¹⁰ , I. Maietto Silverio¹⁰ , P. G. Mercadante¹⁰ , S. F. Novaes¹⁰ , B. Orzari¹⁰ , Sandra S. Padula¹⁰ , V. Scheurer,¹⁰ A. Aleksandrov¹⁰ , G. Antchev¹¹ , P. Danev,¹¹ R. Hadjiiska¹¹ , P. Iaydjiev¹¹ , M. Shopova¹¹ , G. Sultanov¹¹ , A. Dimitrov¹¹ ,¹² L. Litov¹¹ , B. Pavlov¹¹ , P. Petkov¹¹ , A. Petrov¹¹ , S. Keshri¹³ , D. Laroze¹³ , S. Thakur¹³ , W. Brooks¹⁴ , T. Cheng¹⁵ , T. Javaid¹⁵ , L. Wang¹⁵ , L. Yuan¹⁵ , Z. Hu¹⁶ , Z. Liang,¹⁶ J. Liu,¹⁶ X. Wang¹⁶ , G. M. Chen¹⁶ ,^{17,j} H. S. Chen¹⁶ ,^{17,j} M. Chen¹⁶ ,^{17,j} Y. Chen¹⁶ , Q. Hou¹⁷ , X. Hou,¹⁷ F. Iemmi¹⁷ , C. H. Jiang,¹⁷ A. Kapoor^{17,k} , H. Liao¹⁷ , G. Liu¹⁷ , Z.-A. Liu^{17,l} , J. N. Song,^{17,l} S. Song,¹⁷ J. Tao¹⁷ , C. Wang^{17,j} , J. Wang¹⁷ , H. Zhang¹⁷ , J. Zhao¹⁷ , A. Agapitos¹⁸ ,¹⁸ Y. Ban¹⁸ , A. Carvalho Antunes De Oliveira¹⁸ , S. Deng¹⁸ , B. Guo,¹⁸ Q. Guo,¹⁸ C. Jiang¹⁸ , A. Levin¹⁸ , C. Li¹⁸ , Q. Li¹⁸ , Y. Mao,¹⁸ S. Qian,¹⁸ S. J. Qian¹⁸ , X. Qin,¹⁸ C. Quaranta¹⁸ , X. Sun¹⁸ , D. Wang¹⁸ , J. Wang¹⁸ , H. Yang,¹⁸ M. Zhang,¹⁸ Y. Zhao,¹⁸ C. Zhou,¹⁸ S. Yang¹⁹ , Z. You²⁰ , K. Jaffel²¹ , N. Lu²¹ , G. Bauer,^{22,m,n} Z. Cui,^{22,n} B. Li,^{22,o} H. Wang²² , K. Yi^{22,p} , J. Zhang²² , Y. Li,²³ Z. Lin²⁴ , C. Lu²⁴ , M. Xiao^{24,q} , C. Avila²⁵ , D. A. Barbosa Trujillo²⁵ , A. Cabrera²⁵ , C. Florez²⁵ , J. Fraga²⁵ , J. A. Reyes Vega,²⁵ C. Rendón²⁶ , M. Rodriguez²⁶ , A. A. Ruales Barbosa²⁶ , J. D. Ruiz Alvarez²⁶ , N. Godinovic²⁷ , D. Lelas²⁷ , A. Sculac²⁷ , M. Kovac²⁸ , A. Petkovic²⁸ , T. Sculac²⁸ , P. Bargassa²⁹ , V. Brigljevic²⁹ , B. K. Chitroda²⁹ , D. Ferencek²⁹ , K. Jakovcic,²⁹ A. Starodumov²⁹ , T. Susa²⁹ , A. Attikis³⁰ , K. Christoforou³⁰ , A. Hadjiagapiou,³⁰ C. Leonidou³⁰ , C. Nicolaou,³⁰ L. Paizanos³⁰ , F. Ptochos³⁰ , P. A. Razis³⁰ , H. Rykaczewski,³⁰ H. Saka³⁰ , A. Stepennov³⁰ , M. Finger^{31,a} , M. Finger Jr.³¹ , E. Ayala³² , E. Carrera Jarrin³³ , S. Elgammal,^{34,r} A. Ellithi Kamel^{34,s} , A. Hussein,³⁵ H. Mohammed³⁵ , K. Ehataht³⁶ , M. Kadastik³⁶ , T. Lange³⁶ , C. Nielsen³⁶ , J. Pata³⁶ , M. Raidal³⁶ , N. Seeba³⁶ , L. Tani³⁶ , A. Milieva³⁷ , K. Osterberg³⁷ , M. Voutilainen³⁷ , N. Bin Norjoharuddeen³⁸ , E. Brücken³⁸ , F. Garcia³⁸ , P. Inkaew³⁸ , K. T. S. Kallonen³⁸ , R. Kumar Verma³⁸ , T. Lampén³⁸ , K. Lassila-Perini³⁸ , B. Lehtela³⁸ , S. Lehti³⁸ , T. Lindén³⁸ , N. R. Mancilla Xinto³⁸ , M. Myllymäki³⁸ , M. m. Rantanen³⁸ , S. Saariokari³⁸ , N. T. Toikka³⁸ , J. Tuominiemi³⁸ ,³⁸ H. Kirschenmann³⁹ , P. Luukka³⁹ , H. Petrow³⁹ , M. Besancon⁴⁰ , F. Couderc⁴⁰ , M. Dejardin⁴⁰ , D. Denegri,⁴⁰ P. Devoue⁴⁰ , J. L. Faure⁴⁰ , F. Ferri⁴⁰ , P. Gaigne,⁴⁰ S. Ganjour⁴⁰ , P. Gras⁴⁰ , G. Hamel de Monchenault⁴⁰ , M. Kumar⁴⁰ , V. Lohezic⁴⁰ , J. Malcles⁴⁰ , F. Orlandi⁴⁰ , L. Portales⁴⁰ , S. Ronchi⁴⁰ , M. Ö. Sahin,⁴⁰ A. Savoy-Navarro^{40,t} , P. Simkina⁴⁰ , M. Titov⁴⁰ , M. Tornago⁴⁰ , R. Amella Ranz⁴¹ , F. Beaudette⁴¹ , G. Boldrini⁴¹ , P. Busson⁴¹ , C. Charlot⁴¹ , M. Chiusi⁴¹ , T. D. Cuisset⁴¹ , O. Davignon⁴¹ , A. De Wit⁴¹ , T. Debnath⁴¹ , I. T. Ehle⁴¹ ,⁴¹ S. Ghosh⁴¹ , A. Gilbert⁴¹ , R. Granier de Cassagnac⁴¹ , L. Kalipoliti⁴¹ , M. Manoni⁴¹ , M. Nguyen⁴¹ , S. Obraztsov⁴¹ , C. Ochando⁴¹ , R. Salerno⁴¹ , J. B. Sauvan⁴¹ , Y. Sirois⁴¹ , G. Sokmen,⁴¹

N. Chanon⁴⁴, D. Contardo⁴⁴, P. Depasse⁴⁴, H. El Mamouni⁴⁴, J. Fay⁴⁴, S. Gascon⁴⁴, M. Gouzevitch⁴⁴, C. Greenberg⁴⁴, G. Grenier⁴⁴, B. Ille⁴⁴, E. Jourdain⁴⁴, I. B. Laktineh⁴⁴, M. Lethuillier⁴⁴, B. Massoteau⁴⁴, L. Mirabito⁴⁴, A. Purohit⁴⁴, M. Vander Donckt⁴⁴, J. Xiao⁴⁴, G. Adamov⁴⁵, I. Lomidze⁴⁵, Z. Tsamalaidze^{45,v}, V. Botta⁴⁶, S. Consuegra Rodríguez⁴⁶, L. Feld⁴⁶, K. Klein⁴⁶, M. Lipinski⁴⁶, D. Meuser⁴⁶, P. Nattland⁴⁶, V. Oppenländer⁴⁶, A. Pauls⁴⁶, D. Pérez Adán⁴⁶, N. Röwert⁴⁶, M. Teroerde⁴⁶, C. Daumann⁴⁷, S. Diekmann⁴⁷, A. Dodonova⁴⁷, N. Eich⁴⁷, D. Eliseev⁴⁷, F. Engelke⁴⁷, J. Erdmann⁴⁷, M. Erdmann⁴⁷, B. Fischer⁴⁷, T. Hebbeker⁴⁷, K. Hoepfner⁴⁷, F. Ivone⁴⁷, A. Jung⁴⁷, N. Kumar⁴⁷, M. y. Lee⁴⁷, F. Mausolf⁴⁷, M. Merschmeyer⁴⁷, A. Meyer⁴⁷, F. Nowotny⁴⁷, A. Pozdnyakov⁴⁷, W. Redjeb⁴⁷, H. Reithler⁴⁷, U. Sarkar⁴⁷, V. Sarkisovi⁴⁷, A. Schmidt⁴⁷, C. Seth⁴⁷, A. Sharma⁴⁷, J. L. Spah⁴⁷, V. Vaulin⁴⁷, S. Zaleski⁴⁷, M. R. Beckers⁴⁸, C. Dziwok⁴⁸, G. Flügge⁴⁸, N. Hoeflich⁴⁸, T. Kress⁴⁸, A. Nowack⁴⁸, O. Pooth⁴⁸, A. Stahl⁴⁸, A. Zolt⁴⁸, H. Aarup Petersen⁴⁹, A. Abel⁴⁹, M. Aldaya Martin⁴⁹, J. Alimena⁴⁹, S. Amoroso⁴⁹, Y. An⁴⁹, I. Andreev⁴⁹, J. Bach⁴⁹, S. Baxter⁴⁹, M. Bayatmakou⁴⁹, H. Becerril Gonzalez⁴⁹, O. Behnke⁴⁹, A. Belvedere⁴⁹, F. Blekman^{49,w}, K. Borrás^{49,x}, A. Campbell⁴⁹, S. Chatterjee⁴⁹, L. X. Coll Saravia⁴⁹, G. Eckerlin⁴⁹, D. Eckstein⁴⁹, E. Gallo^{49,w}, A. Geiser⁴⁹, V. Guglielmi⁴⁹, M. Guthoff⁴⁹, A. Hinzmann⁴⁹, L. Jeppe⁴⁹, M. Kasemann⁴⁹, C. Kleinwort⁴⁹, R. Kogler⁴⁹, M. Komm⁴⁹, D. Krücker⁴⁹, W. Lange⁴⁹, D. Leyva Pernia⁴⁹, K.-Y. Lin⁴⁹, K. Lipka^{49,y}, W. Lohmann^{49,z}, J. Malvaso⁴⁹, R. Mankel⁴⁹, I.-A. Melzer-Pellmann⁴⁹, M. Mendizabal Morentin⁴⁹, A. B. Meyer⁴⁹, G. Milella⁴⁹, K. Moral Figueroa⁴⁹, A. Mussgiller⁴⁹, L. P. Nair⁴⁹, J. Niedziela⁴⁹, A. Nürnberg⁴⁹, J. Park⁴⁹, E. Ranken⁴⁹, A. Raspereza⁴⁹, D. Rastorguev⁴⁹, L. Rygaard⁴⁹, M. Scham^{49,aa,x}, S. Schnake^{49,x}, P. Schütze⁴⁹, C. Schwanenberger^{49,w}, D. Selivanova⁴⁹, K. Sharke⁴⁹, M. Shchedrolosiev⁴⁹, D. Stafford⁴⁹, M. Torkian⁴⁹, F. Vazzoler⁴⁹, A. Ventura Barroso⁴⁹, R. Walsh⁴⁹, D. Wang⁴⁹, Q. Wang⁴⁹, K. Wichmann⁴⁹, L. Wiens^{49,x}, C. Wissing⁴⁹, Y. Yang⁴⁹, S. Zakharov⁴⁹, A. Zimmermann Castro Santos⁴⁹, A. R. Alves Andrade⁵⁰, M. Antonello⁵⁰, S. Bollweg⁵⁰, M. Bonanomi⁵⁰, K. El Morabit⁵⁰, Y. Fischer⁵⁰, M. Frahm⁵⁰, E. Garutti⁵⁰, A. Grohsjean⁵⁰, A. A. Guvenli⁵⁰, J. Haller⁵⁰, D. Hundhausen⁵⁰, G. Kasieczka⁵⁰, P. Keicher⁵⁰, R. Klanner⁵⁰, W. Korcaric⁵⁰, T. Kramer⁵⁰, C. c. Kuo⁵⁰, F. Labe⁵⁰, J. Lange⁵⁰, A. Lobanov⁵⁰, L. Moureaux⁵⁰, A. Nigamova⁵⁰, K. Nikolopoulos⁵⁰, A. Paasch⁵⁰, K. J. Pena Rodriguez⁵⁰, N. Prouvost⁵⁰, T. Quadfasel⁵⁰, B. Raciti⁵⁰, M. Rieger⁵⁰, D. Savoie⁵⁰, P. Schleper⁵⁰, M. Schröder⁵⁰, J. Schwandt⁵⁰, M. Sommerhalder⁵⁰, H. Stadie⁵⁰, G. Steinbrück⁵⁰, R. Ward⁵⁰, B. Wiederspan⁵⁰, M. Wolf⁵⁰, S. Brommer⁵¹, E. Butz⁵¹, Y. M. Chen⁵¹, T. Chwalek⁵¹, A. Dierlamm⁵¹, G. G. Dincer⁵¹, U. Elicabuk⁵¹, N. Faltermann⁵¹, M. Giffels⁵¹, A. Gottmann⁵¹, F. Hartmann^{51,bb}, M. Horzela⁵¹, F. Hummer⁵¹, U. Husemann⁵¹, J. Kieseler⁵¹, M. Klute⁵¹, R. Kunnilan Muhammed Rafeek⁵¹, O. Lavoryk⁵¹, J. M. Lawhorn⁵¹, A. Lintuluoto⁵¹, S. Maier⁵¹, M. Mormile⁵¹, Th. Müller⁵¹, E. Pfeffer⁵¹, M. Presilla⁵¹, G. Quast⁵¹, K. Rabbertz⁵¹, B. Regnery⁵¹, R. Schmieder⁵¹, N. Shadskiy⁵¹, I. Shvetsov⁵¹, H. J. Simonis⁵¹, L. Sowa⁵¹, L. Stockmeier⁵¹, K. Tauqeer⁵¹, M. Toms⁵¹, B. Topko⁵¹, N. Trevisani⁵¹, C. Verstege⁵¹, T. Voigtländer⁵¹, R. F. Von Cube⁵¹, J. Von Den Driesch⁵¹, M. Wassmer⁵¹, R. Wolf⁵¹, W. D. Zeuner⁵¹, X. Zuo⁵¹, G. Anagnostou⁵², G. Daskalakis⁵², A. Kyriakis⁵², G. Melachroinos⁵³, Z. Painesis⁵³, I. Paraskevas⁵³, N. Saoulidou⁵³, K. Theofilatos⁵³, E. Tziaferi⁵³, E. Tzovara⁵³, K. Vellidis⁵³, I. Zisopoulos⁵³, T. Chatzistavrou⁵⁴, G. Karapostoli⁵⁴, K. Kousouris⁵⁴, E. Siamarkou⁵⁴, G. Tsiopolitis⁵⁴, I. Bestintzanos⁵⁵, I. Evangelou⁵⁵, C. Foudas⁵⁵, P. Katsoulis⁵⁵, P. Kokkas⁵⁵, P. G. Kosmoglou Kioseoglou⁵⁵, N. Manthos⁵⁵, I. Papadopoulos⁵⁵, J. Strologas⁵⁵, D. Druzhkin⁵⁶, C. Hajdu⁵⁶, D. Horvath^{56,cc,dd}, K. Márton⁵⁶, A. J. Rádl^{56,ee}, F. Sikler⁵⁶, V. Veszpremi⁵⁶, M. Csanád⁵⁷, K. Farkas⁵⁷, A. Fehérkúti^{57,ff}, M. M. A. Gadallah^{57,gg}, Á. Kadlecik⁵⁷, M. León Coello⁵⁷, G. Pásztor⁵⁷, G. I. Veres⁵⁷, B. Ujvari⁵⁸, G. Zilizi⁵⁸, G. Bencze⁵⁹, S. Czellar⁵⁹, J. Molnar⁵⁹, Z. Szillasi⁵⁹, T. Csorgo^{60,ff}, F. Nemes^{60,ff}, T. Novak⁶⁰, I. Szanyi^{60,hh}, S. Bansal⁶¹, S. B. Beri⁶¹, V. Bhatnagar⁶¹, G. Chaudhary⁶¹, S. Chauhan⁶¹, N. Dhingra^{61,ii}, A. Kaur⁶¹, A. Kaur⁶¹, H. Kaur⁶¹, M. Kaur⁶¹, S. Kumar⁶¹, T. Sheokand⁶¹, J. B. Singh⁶¹, A. Singla⁶¹, A. Bhardwaj⁶², A. Chhetri⁶², B. C. Choudhary⁶², A. Kumar⁶², A. Kumar⁶², M. Naimuddin⁶², S. Phor⁶², K. Ranjan⁶², M. K. Saini⁶², S. Acharya^{63,ji}, B. Gomber⁶³, B. Sahu^{63,jj}, S. Mukherjee⁶⁴, S. Baradia⁶⁵, S. Bhattacharya⁶⁵, S. Das Gupta⁶⁵, S. Dutta⁶⁵, S. Dutta⁶⁵, S. Sarkar⁶⁵, M. M. Ameen⁶⁶, P. K. Behera⁶⁶, S. Chatterjee⁶⁶, G. Dash⁶⁶, A. Dattamunsi⁶⁶, P. Jana⁶⁶, P. Kalbhor⁶⁶, S. Kamble⁶⁶, J. R. Komaragiri^{66,kk}, T. Mishra⁶⁶, P. R. Pujahari⁶⁶, A. K. Sikdar⁶⁶, R. K. Singh⁶⁶, P. Verma⁶⁶, S. Verma⁶⁶, A. Vijay⁶⁶, B. K. Sirasva⁶⁷, L. Bhatt⁶⁸, S. Dugad⁶⁸, G. B. Mohanty⁶⁸, M. Shelake⁶⁸, P. Suryadevara⁶⁸, A. Bala⁶⁹, S. Banerjee⁶⁹, S. Barman^{69,ll}, R. M. Chatterjee⁶⁹, M. Guchait⁶⁹, Sh. Jain⁶⁹, A. Jaiswal⁶⁹, B. M. Joshi⁶⁹

S. Kumar⁶⁹, M. Maity^{69,II}, G. Majumder⁶⁹, K. Mazumdar⁶⁹, S. Parolia⁶⁹, R. Saxena⁶⁹, A. Thachayath⁶⁹,
 S. Bahinipati^{70,mm}, D. Maity^{70,nn}, P. Mal⁷⁰, K. Naskar^{70,nn}, A. Nayak^{70,nn}, S. Nayak⁷⁰, K. Pal⁷⁰, R. Raturi,⁷⁰
 P. Sadangi,⁷⁰ S. K. Swain⁷⁰, S. Varghese^{70,nn}, D. Vats^{70,nn}, A. Alpana⁷¹, S. Dube⁷¹, P. Hazarika⁷¹, B. Kansal⁷¹,
 A. Laha⁷¹, R. Sharma⁷¹, S. Sharma⁷¹, K. Y. Vaish⁷¹, S. Ghosh⁷², H. Bakhshiansohi^{73,oo}, A. Jafari^{73,pp},
 V. Sedighzadeh Dalavi⁷³, M. Zeinali^{73,qq}, S. Bashiri⁷⁴, S. Chenarani^{74,rr}, S. M. Etesami⁷⁴, Y. Hosseini⁷⁴,
 M. Khakzad⁷⁴, E. Khazaie⁷⁴, M. Mohammadi Najafabadi⁷⁴, S. Tizchang^{74,ss}, M. Felcini⁷⁵, M. Grunewald⁷⁵,
 M. Abbrescia^{76a,76b}, M. Barbieri^{76a,76b}, M. Buonsante^{76a,76b}, A. Colaleo^{76a,76b}, D. Creanza^{76a,76c},
 N. De Filippis^{76a,76c}, M. De Palma^{76a,76b}, W. Elmetenawee^{76a,76b,tt}, N. Ferrara^{76a,76c}, L. Fiore^{76a}, L. Longo^{76a},
 M. Louka^{76a,76b}, G. Maggi^{76a,76c}, M. Maggi^{76a}, I. Margjeka^{76a}, V. Mastrapasqua^{76a,76b}, S. My^{76a,76b},
 F. Nenna^{76a,76b}, S. Nuzzo^{76a,76b}, A. Pellecchia^{76a,76b}, A. Pompili^{76a,76b}, G. Pugliese^{76a,76c}, R. Radogna^{76a,76b},
 D. Ramos^{76a}, A. Ranieri^{76a}, L. Silvestris^{76a}, F. M. Simone^{76a,76c}, Ü. Sözbilir^{76a}, A. Stamerra^{76a,76b},
 D. Troiano^{76a,76b}, R. Venditti^{76a,76b}, P. Verwilligen^{76a}, A. Zaza^{76a,76b}, G. Abbiendi^{77a}, C. Battilana^{77a,77b},
 D. Bonacorsi^{77a,77b}, P. Capiluppi^{77a,77b}, F. R. Cavallo^{77a}, M. Cuffiani^{77a,77b}, G. M. Dallavalle^{77a}, T. Diotalevi^{77a,77b},
 F. Fabbri^{77a}, A. Fanfani^{77a,77b}, P. Giacomelli^{77a}, L. Giommi^{77a,77b}, C. Grandi^{77a}, L. Guiducci^{77a,77b},
 S. Lo Meo^{77a,uu}, M. Lorusso^{77a,77b}, L. Lunerti^{77a}, S. Marcellini^{77a}, F. L. Navarria^{77a,77b}, G. Paggi^{77a,77b},
 A. Perrotta^{77a}, F. Primavera^{77a,77b}, A. M. Rossi^{77a,77b}, S. Rossi Tisbeni^{77a,77b}, T. Rovelli^{77a,77b}, G. P. Siroli^{77a,77b},
 S. Costa^{78a,78b,vv}, A. Di Mattia^{78a}, A. Lapertosa^{78a}, R. Potenza^{78a,78b}, A. Tricomi^{78a,78b,vv}, J. Altork^{79a,79b},
 P. Assiouras^{79a}, G. Barbagli^{79a}, G. Bardelli^{79a}, M. Bartolini^{79a,79b}, A. Calandri^{79a,79b}, B. Camaiani^{79a,79b},
 A. Cassese^{79a}, R. Ceccarelli^{79a}, V. Ciulli^{79a,79b}, C. Civinini^{79a}, R. D'Alessandro^{79a,79b}, L. Damenti,^{79a,79b}
 E. Focardi^{79a,79b}, T. Kello^{79a}, G. Latino^{79a,79b}, P. Lenzi^{79a,79b}, M. Lizzo^{79a}, M. Meschini^{79a}, S. Paoletti^{79a},
 A. Papanastassiou,^{79a,79b} G. Sguazzoni^{79a}, L. Viliani^{79a}, L. Benussi⁸⁰, S. Bianco⁸⁰, S. Meola^{80,ww}, D. Piccolo⁸⁰,
 M. Alves Gallo Pereira^{81a}, F. Ferro^{81a}, E. Robutti^{81a}, S. Tosi^{81a,81b}, A. Benaglia^{82a}, F. Brivio^{82a},
 V. Camagni^{82a,82b}, F. Cetorelli^{82a,82b}, F. De Guio^{82a,82b}, M. E. Dinardo^{82a,82b}, P. Dini^{82a}, S. Gennai^{82a},
 R. Gerosa^{82a,82b}, A. Ghezzi^{82a,82b}, P. Govoni^{82a,82b}, L. Guzzi^{82a}, M. R. Kim^{82a}, G. Lavizzari,^{82a,82b}
 M. T. Lucchini^{82a,82b}, M. Malberti^{82a}, S. Malvezzi^{82a}, A. Massironi^{82a}, D. Menasce^{82a}, L. Moroni^{82a},
 M. Paganoni^{82a,82b}, S. Palluotto^{82a,82b}, D. Pedrini^{82a}, A. Perego^{82a,82b}, G. Pizzati^{82a,82b}, S. Ragazzi^{82a,82b},
 T. Tabarelli de Fatis^{82a,82b}, S. Buontempo^{83a}, C. Di Fraia^{83a,83b}, F. Fabozzi^{83a,83c}, L. Favilla^{83a,83d},
 A. O. M. Iorio^{83a,83b}, L. Lista^{83a,83b,xx}, P. Paolucci^{83a,bb}, B. Rossi^{83a}, P. Azzi^{84a}, N. Bacchetta^{84a,yy},
 D. Bisello^{84a,84b}, P. Bortignon^{84a,84c}, G. Bortolato^{84a,84b}, A. C. M. Bulla^{84a,84c}, R. Carlin^{84a,84b}, P. Checchia^{84a},
 T. Dorigo^{84a,zz}, U. Gasparini^{84a,84b}, S. Giorgetti^{84a}, F. Gonella^{84a}, E. Lusiani^{84a}, M. Margoni^{84a,84b},
 A. T. Meneguzzo^{84a,84b}, J. Pazzini^{84a,84b}, P. Ronchese^{84a,84b}, R. Rossin^{84a,84b}, F. Simonetto^{84a,84b}, M. Tosi^{84a,84b},
 A. Triossi^{84a,84b}, M. Zanetti^{84a,84b}, P. Zotto^{84a,84b}, A. Zucchetta^{84a,84b}, G. Zumerle^{84a,84b}, A. Braghieri^{85a},
 S. Calzaferri^{85a}, P. Montagna^{85a,85b}, M. Pelliccioni^{85a}, V. Re^{85a}, C. Riccardi^{85a,85b}, P. Salvini^{85a}, I. Vai^{85a,85b},
 P. Vitulo^{85a,85b}, S. Ajmal^{86a,86b}, M. E. Ascoti^{86a,86b}, G. M. Bilei^{86a}, C. Carrivale,^{86a,86b} D. Ciangottini^{86a,86b},
 L. Della Penna,^{86a,86b} L. Fanò^{86a,86b}, V. Mariani^{86a,86b}, M. Menichelli^{86a}, F. Moscatelli^{86a,aaa}, A. Rossi^{86a,86b},
 A. Santocchia^{86a,86b}, D. Spiga^{86a}, T. Tedeschi^{86a,86b}, C. Aimè^{87a,87b}, C. A. Alexe^{87a,87c}, P. Asenov^{87a,87b},
 P. Azzurri^{87a}, G. Bagliesi^{87a}, R. Bhattacharya^{87a}, L. Bianchini^{87a,87b}, T. Boccali^{87a}, E. Bossini^{87a},
 D. Bruschini^{87a,87c}, L. Calligaris^{87a,87b}, R. Castaldi^{87a}, F. Cattafesta^{87a,87c}, M. A. Ciocci^{87a,87d}, M. Cipriani^{87a,87b},
 R. Dell'Orso^{87a}, S. Donato^{87a,87b}, R. Forti^{87a,87b}, A. Giassi^{87a}, F. Ligabue^{87a,87c}, A. C. Marini^{87a,87b},
 D. Matos Figueiredo^{87a}, A. Messineo^{87a,87b}, S. Mishra^{87a}, V. K. Muraleedharan Nair Bindhu^{87a,87b}, S. Nandan^{87a},
 F. Palla^{87a}, M. Riggirello^{87a,87c}, A. Rizzi^{87a,87b}, G. Rolandi^{87a,87c}, S. Roy Chowdhury^{87a,bbb}, T. Sarkar^{87a},
 A. Scribano^{87a}, P. Solanki^{87a,87b}, P. Spagnolo^{87a}, F. Tenchini^{87a,87b}, R. Tenchini^{87a}, G. Tonelli^{87a,87b},
 N. Turini^{87a,87d}, F. Vaselli^{87a,87c}, A. Venturi^{87a}, P. G. Verdini^{87a}, P. Akrap^{88a,88b}, C. Basile^{88a,88b}, S. C. Behera^{88a},
 F. Cavallari^{88a}, L. Cunqueiro Mendez^{88a,88b}, F. De Ruggi^{88a,88b}, D. Del Re^{88a,88b}, E. Di Marco^{88a}, M. Diemoz^{88a},
 F. Errico^{88a}, L. Frosina^{88a,88b}, R. Gargiulo^{88a,88b}, B. Harikrishnan^{88a,88b}, F. Lombardi,^{88a,88b} E. Longo^{88a,88b},
 L. Martikainen^{88a,88b}, J. Mijuskovic^{88a,88b}, G. Organtini^{88a,88b}, N. Palmeri^{88a,88b}, R. Paramatti^{88a,88b},
 S. Rahatlou^{88a,88b}, C. Rovelli^{88a}, F. Santanastasio^{88a,88b}, L. Soffi^{88a}, V. Vladimirov,^{88a,88b} N. Amapane^{89a,89b},
 R. Arcidiacono^{89a,89c}, S. Argiro^{89a,89b}, M. Arneodo^{89a,89c}, N. Bartosik^{89a,89c}, R. Bellan^{89a,89b}, A. Bellora^{89a,89b},
 C. Biino^{89a}, C. Borca^{89a,89b}, N. Cartiglia^{89a}, M. Costa^{89a,89b}, R. Covarelli^{89a,89b}, N. Demaria^{89a}, L. Finco^{89a}

M. Grippo^{89a,89b} B. Kiani^{89a,89b} L. Lanteri^{89a,89b} F. Legger^{89a} F. Luongo^{89a,89b} C. Mariotti^{89a} S. Maselli^{89a}
 A. Mecca^{89a,89b} L. Menzio^{89a,89b} P. Meridiani^{89a} E. Migliore^{89a,89b} M. Monteno^{89a} M. M. Obertino^{89a,89b}
 G. Ortona^{89a} L. Pacher^{89a,89b} N. Pastrone^{89a} M. Ruspa^{89a,89c} F. Siviero^{89a,89b} V. Sola^{89a,89b} A. Solano^{89a,89b}
 A. Staiano^{89a} C. Tarricone^{89a,89b} D. Trocino^{89a} G. Umoret^{89a,89b} E. Vlasov^{89a,89b} R. White^{89a,89b}
 J. Babbar^{90a,90b} S. Belforte^{90a} V. Candelise^{90a,90b} M. Casarsa^{90a} F. Cossutti^{90a} K. De Leo^{90a}
 G. Della Ricca^{90a,90b} R. Delli Gatti^{90a,90b} S. Dogra⁹¹ J. Hong⁹¹ J. Kim⁹¹ T. Kim⁹¹ D. Lee⁹¹ H. Lee⁹¹
 J. Lee⁹¹ S. W. Lee⁹¹ C. S. Moon⁹¹ Y. D. Oh⁹¹ S. Sekmen⁹¹ B. Tae⁹¹ Y. C. Yang⁹¹ M. S. Kim⁹² G. Bak⁹³
 P. Gwak⁹³ H. Kim⁹³ D. H. Moon⁹³ J. Seo⁹³ E. Asilar⁹⁴ F. Carnevali⁹⁴ J. Choi^{94,ccc} T. J. Kim⁹⁴ Y. Ryou⁹⁴
 S. Ha⁹⁵ S. Han⁹⁵ B. Hong⁹⁵ J. Kim⁹⁵ K. Lee⁹⁵ K. S. Lee⁹⁵ S. Lee⁹⁵ J. Yoo⁹⁵ J. Goh⁹⁶ J. Shin⁹⁶
 S. Yang⁹⁶ Y. Kang⁹⁷ H. S. Kim⁹⁷ Y. Kim⁹⁷ S. Lee⁹⁷ J. Almond⁹⁸ J. H. Bhyun⁹⁸ J. Choi⁹⁸ J. Choi⁹⁸ W. Jun⁹⁸
 H. Kim⁹⁸ J. Kim⁹⁸ T. Kim⁹⁸ Y. Kim⁹⁸ Y. W. Kim⁹⁸ S. Ko⁹⁸ H. Lee⁹⁸ J. Lee⁹⁸ J. Lee⁹⁸ B. H. Oh⁹⁸
 S. B. Oh⁹⁸ J. Shin⁹⁸ U. K. Yang⁹⁸ I. Yoon⁹⁸ W. Jang⁹⁹ D. Y. Kang⁹⁹ D. Kim⁹⁹ S. Kim⁹⁹ B. Ko⁹⁹
 J. S. H. Lee⁹⁹ Y. Lee⁹⁹ I. C. Park⁹⁹ Y. Roh⁹⁹ I. J. Watson⁹⁹ G. Cho¹⁰⁰ K. Hwang¹⁰⁰ B. Kim¹⁰⁰ S. Kim¹⁰⁰
 K. Lee¹⁰⁰ H. D. Yoo¹⁰⁰ M. Choi¹⁰¹ Y. Lee¹⁰¹ I. Yu¹⁰¹ T. Beyrouthy¹⁰² Y. Gharbia¹⁰² F. Alazemi¹⁰³
 K. Dreimanis¹⁰⁴ O. M. Eberlins¹⁰⁴ A. Gaile¹⁰⁴ C. Munoz Diaz¹⁰⁴ D. Osite¹⁰⁴ G. Pikurs¹⁰⁴ R. Plese¹⁰⁴
 A. Potrebko¹⁰⁴ M. Seidel¹⁰⁴ D. Sidiropoulos Kontos¹⁰⁴ N. R. Strautnieks¹⁰⁵ M. Ambrozias¹⁰⁶
 A. Juodagalvis¹⁰⁶ S. Nargelas¹⁰⁶ A. Rinkevicius¹⁰⁶ G. Tamulaitis¹⁰⁶ I. Yusuff^{107,ddd} Z. Zolkapli¹⁰⁷
 J. F. Benitez¹⁰⁸ A. Castaneda Hernandez¹⁰⁸ A. Cota Rodriguez¹⁰⁸ L. E. Cuevas Picos¹⁰⁸ H. A. Encinas Acosta¹⁰⁸
 L. G. Gallegos Maríñez¹⁰⁸ J. A. Murillo Quijada¹⁰⁸ L. Valencia Palomo¹⁰⁸ G. Ayala¹⁰⁹ H. Castilla-Valdez¹⁰⁹
 H. Crotte Ledesma¹⁰⁹ R. Lopez-Fernandez¹⁰⁹ J. Mejia Guisao¹⁰⁹ R. Reyes-Almanza¹⁰⁹
 A. Sánchez Hernández¹⁰⁹ C. Oropeza Barrera¹¹⁰ D. L. Ramirez Guadarrama¹¹⁰ M. Ramírez García¹¹⁰
 I. Bautista¹¹¹ F. E. Neri Huerta¹¹¹ I. Pedraza¹¹¹ H. A. Salazar Ibarguen¹¹¹ C. Uribe Estrada¹¹¹ I. Bujanja¹¹²
 N. Raicevic¹¹² P. H. Butler¹¹³ A. Ahmad¹¹⁴ M. I. Asghar¹¹⁴ A. Awais¹¹⁴ M. I. M. Awan¹¹⁴ W. A. Khan¹¹⁴
 V. Avati¹¹⁵ L. Forthomme¹¹⁵ L. Grzanka¹¹⁵ M. Malawski¹¹⁵ K. Piotrkowski¹¹⁵ M. Bluj¹¹⁶ M. Górski¹¹⁶
 M. Kazana¹¹⁶ M. Szeleper¹¹⁶ P. Zalewski¹¹⁶ K. Bunkowski¹¹⁷ K. Doroba¹¹⁷ A. Kalinowski¹¹⁷ M. Konecki¹¹⁷
 J. Krolikowski¹¹⁷ A. Muhammad¹¹⁷ P. Fokow¹¹⁸ K. Pozniak¹¹⁸ W. Zabolotny¹¹⁸ M. Araujo¹¹⁹ D. Bastos¹¹⁹
 C. Beirão Da Cruz E Silva¹¹⁹ A. Boletti¹¹⁹ M. Bozzo¹¹⁹ T. Camporesi¹¹⁹ G. Da Molin¹¹⁹ M. Gallinaro¹¹⁹
 J. Hollar¹¹⁹ N. Leonardo¹¹⁹ G. B. Marozzo¹¹⁹ A. Petrilli¹¹⁹ M. Pisano¹¹⁹ J. Seixas¹¹⁹ J. Varela¹¹⁹
 J. W. Wulff¹¹⁹ P. Adzic¹²⁰ L. Markovic¹²⁰ P. Milenovic¹²⁰ V. Milosevic¹²⁰ D. Devetak¹²¹ M. Dordevic¹²¹
 J. Milosevic¹²¹ L. Nadder¹²¹ V. Rekovic¹²¹ M. Stojanovic¹²¹ M. Alcalde Martinez¹²² J. Alcaraz Maestre¹²²
 Cristina F. Bedoya¹²² J. A. Brochero Cifuentes¹²² Oliver M. Carretero¹²² M. Cepeda¹²² M. Cerrada¹²²
 N. Colino¹²² J. Cuchillo Ortega¹²² B. De La Cruz¹²² A. Delgado Peris¹²² A. Escalante Del Valle¹²²
 D. Fernández Del Val¹²² J. P. Fernández Ramos¹²² J. Flix¹²² M. C. Fouz¹²² M. Gonzalez Hernandez¹²²
 O. Gonzalez Lopez¹²² S. Goy Lopez¹²² J. M. Hernandez¹²² M. I. Josa¹²² J. Llorente Merino¹²²
 C. Martin Perez¹²² E. Martin Viscasillas¹²² D. Moran¹²² C. M. Morcillo Perez¹²² R. Paz Herrera¹²²
 C. Perez Dengra¹²² A. Pérez-Calero Yzquierdo¹²² J. Puerta Pelayo¹²² I. Redondo¹²² J. Vazquez Escobar¹²²
 J. F. de Trocóniz¹²³ B. Alvarez Gonzalez¹²⁴ J. Ayllon Torresano¹²⁴ A. Cardini¹²⁴ J. Cuevas¹²⁴
 J. Del Riego Badas¹²⁴ D. Estrada Acevedo¹²⁴ J. Fernandez Menendez¹²⁴ S. Folgueras¹²⁴
 I. Gonzalez Caballero¹²⁴ P. Leguina¹²⁴ M. Obeso Menendez¹²⁴ E. Palencia Cortezon¹²⁴ J. Prado Pico¹²⁴
 A. Soto Rodríguez¹²⁴ C. Vico Villalba¹²⁴ P. Vischia¹²⁴ S. Blanco Fernández¹²⁵ I. J. Cabrillo¹²⁵ A. Calderon¹²⁵
 J. Duarte Campderros¹²⁵ M. Fernandez¹²⁵ G. Gomez¹²⁵ C. Lasasoa García¹²⁵ R. Lopez Ruiz¹²⁵
 C. Martinez Rivero¹²⁵ P. Martinez Ruiz del Arbol¹²⁵ F. Matorras¹²⁵ P. Matorras Cuevas¹²⁵
 E. Navarrete Ramos¹²⁵ J. Piedra Gomez¹²⁵ C. Quintana San Emeterio¹²⁵ L. Scodellaro¹²⁵ I. Vila¹²⁵
 R. Vilar Cortabitarte¹²⁵ J. M. Vizan Garcia¹²⁵ B. Kailasapathy^{126,eee} D. D. C. Wickramaratna¹²⁶
 W. G. D. Dharmaratna^{127,fff} K. Liyanage¹²⁷ N. Perera¹²⁷ D. Abbaneo¹²⁸ C. Amendola¹²⁸ R. Ardino¹²⁸
 E. Auffray¹²⁸ J. Baechler¹²⁸ D. Barney¹²⁸ J. Bendavid¹²⁸ M. Bianco¹²⁸ A. Bocci¹²⁸ L. Borgonovi¹²⁸
 C. Botta¹²⁸ A. Bragagnolo¹²⁸ C. E. Brown¹²⁸ C. Caillol¹²⁸ G. Cerminara¹²⁸ P. Connor¹²⁸ D. d'Enterria¹²⁸
 A. Dabrowski¹²⁸ A. David¹²⁸ A. De Roeck¹²⁸ M. M. Defranchis¹²⁸ M. Deile¹²⁸ M. Dobson¹²⁸
 P. J. Fernández Manteca¹²⁸ B. A. Fontana Santos Alves¹²⁸ W. Funk¹²⁸ A. Gaddi¹²⁸ S. Giani¹²⁸ D. Gigi¹²⁸

K. Gill¹²⁸, F. Glege¹²⁸, M. Glowacki¹²⁸, A. Gruber¹²⁸, J. Hegeman¹²⁸, J. K. Heikkilä¹²⁸, R. Hofsaess¹²⁸,
 B. Huber¹²⁸, T. James¹²⁸, P. Janot¹²⁸, O. Kaluzinska¹²⁸, O. Karacheban^{128,z}, G. Karathanasis¹²⁸, S. Laurila¹²⁸,
 P. Lecoq¹²⁸, C. Lourenço¹²⁸, A.-M. Lyon¹²⁸, M. Magherini¹²⁸, L. Malgeri¹²⁸, M. Mannelli¹²⁸, A. Mehta¹²⁸,
 F. Meijers¹²⁸, J. A. Merlin¹²⁸, S. Mersi¹²⁸, E. Meschi¹²⁸, M. Migliorini¹²⁸, F. Monti¹²⁸, F. Moortgat¹²⁸,
 M. Mulders¹²⁸, M. Musich¹²⁸, I. Neutelings¹²⁸, S. Orfanelli¹²⁸, F. Pantaleo¹²⁸, M. Pari¹²⁸, G. Petrucciani¹²⁸,
 A. Pfeiffer¹²⁸, M. Pierini¹²⁸, M. Pitt¹²⁸, H. Qu¹²⁸, D. Rabady¹²⁸, A. Reimers¹²⁸, B. Ribeiro Lopes¹²⁸, F. Riti¹²⁸,
 P. Rosado¹²⁸, M. Rovere¹²⁸, H. Sakulin¹²⁸, R. Salvatico¹²⁸, S. Sanchez Cruz¹²⁸, S. Scarfi¹²⁸, M. Selvaggi¹²⁸,
 A. Sharma¹²⁸, K. Shchelina¹²⁸, P. Silva¹²⁸, P. Sphicas^{128,ggg}, A. G. Stahl Leiton¹²⁸, A. Steen¹²⁸, S. Summers¹²⁸,
 D. Treille¹²⁸, P. Tropea¹²⁸, E. Vernazza¹²⁸, J. Wanczyk^{128,hhh}, J. Wang¹²⁸, S. Wuchterl¹²⁸, M. Zarucki¹²⁸,
 P. Zehetner¹²⁸, P. Zejdl¹²⁸, G. Zevi Della Porta¹²⁸, T. Bevilacqua^{128,iii}, L. Caminada^{128,iii}, W. Erdmann¹²⁹,
 R. Horisberger¹²⁹, Q. Ingram¹²⁹, H. C. Kaestli¹²⁹, D. Kotlinski¹²⁹, C. Lange¹²⁹, U. Langenegger¹²⁹,
 L. Nohte^{129,iii}, T. Rohe¹²⁹, A. Samalan¹²⁹, T. K. Aarrestad¹³⁰, M. Backhaus¹³⁰, G. Bonomelli¹³⁰,
 C. Cazzaniga¹³⁰, K. Datta¹³⁰, P. De Bryas Dexmiers D'Archiacchiac^{130,hhh}, A. De Cosa¹³⁰, G. Dissertori¹³⁰,
 M. Dittmar¹³⁰, M. Donegà¹³⁰, F. Eble¹³⁰, K. Gedia¹³⁰, F. Glessgen¹³⁰, C. Grab¹³⁰, N. Härringer¹³⁰,
 T. G. Harte¹³⁰, W. Lustermaun¹³⁰, M. Malucchi¹³⁰, R. A. Manzoni¹³⁰, M. Marchegiani¹³⁰, L. Marchese¹³⁰,
 A. Mascellani^{130,hhh}, F. Nessi-Tedaldi¹³⁰, F. Pauss¹³⁰, V. Perovic¹³⁰, B. Ristic¹³⁰, R. Seidita¹³⁰,
 J. Steggemann^{130,hhh}, A. Tarabini¹³⁰, D. Valsecchi¹³⁰, R. Wallny¹³⁰, C. Amsler^{131,ijj}, P. Bäertschi¹³¹,
 F. Bilandzija¹³¹, M. F. Canelli¹³¹, G. Celotto¹³¹, K. Cormier¹³¹, M. Huwiler¹³¹, W. Jin¹³¹, A. Jofrehei¹³¹,
 B. Kilminster¹³¹, T. H. Kwok¹³¹, S. Leontsinis¹³¹, V. Lukashenko¹³¹, A. Macchiolo¹³¹, F. Meng¹³¹,
 M. Missiroli¹³¹, J. Motta¹³¹, P. Robmann¹³¹, M. Senger¹³¹, E. Shokr¹³¹, F. Stäger¹³¹, R. Tramontano¹³¹,
 P. Viscone¹³¹, D. Bhowmik¹³², C. M. Kuo¹³², P. K. Rout¹³², S. Taj¹³², P. C. Tiwari^{132,kk}, L. Ceard¹³³, K. F. Chen¹³³,
 Z. g. Chen¹³³, A. De Iorio¹³³, W.-S. Hou¹³³, T. h. Hsu¹³³, Y. w. Kao¹³³, S. Karmakar¹³³, G. Kole¹³³, Y. y. Li¹³³,
 R.-S. Lu¹³³, E. Paganis¹³³, X. f. Su¹³³, J. Thomas-Wilsker¹³³, L. s. Tsai¹³³, D. Tsonou¹³³, H. y. Wu¹³³,
 E. Yazgan¹³³, C. Asawatangtrakuldee¹³⁴, N. Srimanobhas¹³⁴, Y. Maghrbi¹³⁵, D. Agyel¹³⁶, F. Dolek¹³⁶,
 I. Dumanoglu^{136,kkk}, Y. Guler^{136,lll}, E. Gurpinar Guler^{136,lll}, C. Isik¹³⁶, O. Kara¹³⁶, A. Kayis Topaksu¹³⁶,
 Y. Komurcu¹³⁶, G. Onengut¹³⁶, K. Ozdemir^{136,mmm}, B. Tali^{136,nnn}, U. G. Tok¹³⁶, E. Uslan¹³⁶, I. S. Zorbakir¹³⁶,
 M. Yalvac^{137,ooo}, B. Akgun¹³⁸, I. O. Atakisi^{138,ppp}, E. Gülmez¹³⁸, M. Kaya^{138,qqq}, O. Kaya^{138,rrr},
 M. A. Sarkisla^{138,sss}, S. Tekten^{138,ttt}, A. Cakir¹³⁹, K. Cankocak^{139,kkk,uuu}, S. Sen^{139,vvv}, B. Haciasahinoglu¹⁴⁰,
 I. Hos^{140,www}, B. Kaynak¹⁴⁰, S. Ozkorucuklu¹⁴⁰, O. Potok¹⁴⁰, H. Sert¹⁴⁰, C. Simsek¹⁴⁰, C. Zorbilmez¹⁴⁰,
 S. Cerci¹⁴¹, C. Dozen^{141,xxx}, B. Isildak^{141,yyy}, E. Simsek¹⁴¹, D. Sunar Cerci¹⁴¹, T. Yetkin^{141,xxx},
 A. Boyaryntsev¹⁴², O. Dadazhanova¹⁴², B. Grynyov¹⁴², L. Levchuk¹⁴³, J. J. Brooke¹⁴⁴, A. Bundock¹⁴⁴,
 F. Bury¹⁴⁴, E. Clement¹⁴⁴, D. Cussans¹⁴⁴, D. Dharmender¹⁴⁴, H. Flacher¹⁴⁴, J. Goldstein¹⁴⁴, H. F. Heath¹⁴⁴,
 M.-L. Holmberg¹⁴⁴, L. Kreczko¹⁴⁴, S. Paramesvaran¹⁴⁴, L. Robertshaw¹⁴⁴, M. S. Sanjrani^{144,oo}, J. Segal¹⁴⁴,
 V. J. Smith¹⁴⁴, A. H. Ball¹⁴⁵, K. W. Bell¹⁴⁵, A. Belyaev^{145,zzz}, C. Brew¹⁴⁵, R. M. Brown¹⁴⁵, D. J. A. Cockerill¹⁴⁵,
 A. Elliot¹⁴⁵, K. V. Ellis¹⁴⁵, J. Gajownik¹⁴⁵, K. Harder¹⁴⁵, S. Harper¹⁴⁵, J. Linacre¹⁴⁵, K. Manolopoulos¹⁴⁵,
 M. Moallemi¹⁴⁵, D. M. Newbold¹⁴⁵, E. Olaiya¹⁴⁵, D. Petyt¹⁴⁵, T. Reis¹⁴⁵, A. R. Sahasransu¹⁴⁵, G. Salvi¹⁴⁵,
 T. Schuh¹⁴⁵, C. H. Shepherd-Themistocleous¹⁴⁵, I. R. Tomalin¹⁴⁵, K. C. Whalen¹⁴⁵, T. Williams¹⁴⁵, I. Andreou¹⁴⁶,
 R. Bainbridge¹⁴⁶, P. Bloch¹⁴⁶, O. Buchmuller¹⁴⁶, C. A. Carrillo Montoya¹⁴⁶, D. Colling¹⁴⁶, J. S. Dancu¹⁴⁶, I. Das¹⁴⁶,
 P. Dauncey¹⁴⁶, G. Davies¹⁴⁶, M. Della Negra¹⁴⁶, S. Fayer¹⁴⁶, G. Fedi¹⁴⁶, G. Hall¹⁴⁶, H. R. Hoorani¹⁴⁶,
 A. Howard¹⁴⁶, G. Iles¹⁴⁶, C. R. Knight¹⁴⁶, P. Krueper¹⁴⁶, J. Langford¹⁴⁶, K. H. Law¹⁴⁶, J. León Holgado¹⁴⁶,
 E. Leutgeb¹⁴⁶, L. Lyons¹⁴⁶, A.-M. Magnan¹⁴⁶, B. Maier¹⁴⁶, S. Mallios¹⁴⁶, A. Mastronikolis¹⁴⁶,
 M. Mieskolainen¹⁴⁶, J. Nash^{146,aaaa}, M. Pesaresi¹⁴⁶, P. B. Pradeep¹⁴⁶, B. C. Radburn-Smith¹⁴⁶, A. Richards¹⁴⁶,
 A. Rose¹⁴⁶, L. Russell¹⁴⁶, K. Savva¹⁴⁶, C. Seez¹⁴⁶, R. Shukla¹⁴⁶, A. Tapper¹⁴⁶, K. Uchida¹⁴⁶, G. P. Uttley¹⁴⁶,
 T. Virdee^{146,bb}, M. Vojinovic¹⁴⁶, N. Wardle¹⁴⁶, D. Winterbottom¹⁴⁶, J. E. Cole¹⁴⁷, A. Khan¹⁴⁷, P. Kyberd¹⁴⁷,
 I. D. Reid¹⁴⁷, S. Abdullin¹⁴⁸, A. Brinkerhoff¹⁴⁸, E. Collins¹⁴⁸, M. R. Darwish¹⁴⁸, J. Dittmann¹⁴⁸,
 K. Hatakeyama¹⁴⁸, V. Hegde¹⁴⁸, J. Hiltbrand¹⁴⁸, B. McMaster¹⁴⁸, J. Samudio¹⁴⁸, S. Sawant¹⁴⁸,
 C. Sutantawibul¹⁴⁸, J. Wilson¹⁴⁸, J. M. Hogan^{149,bbbb}, R. Bartek¹⁵⁰, A. Dominguez¹⁵⁰, S. Raj¹⁵⁰,
 A. E. Simsek¹⁵⁰, S. S. Yu¹⁵⁰, B. Bam¹⁵¹, A. Buchot Perraguin¹⁵¹, S. Campbell¹⁵¹, R. Chudasama¹⁵¹,
 S. I. Cooper¹⁵¹, C. Crovella¹⁵¹, G. Fidalgo¹⁵¹, S. V. Gleyzer¹⁵¹, A. Khukhunaishvili¹⁵¹, K. Matchev¹⁵¹

E. Pearson,¹⁵¹ C. U. Perez,¹⁵¹ P. Rumerio,^{151,cccc} E. Usai,¹⁵¹ R. Yi,¹⁵¹ S. Cholak,¹⁵² G. De Castro,¹⁵²
 Z. Demiragli,¹⁵² C. Erice,¹⁵² C. Fangmeier,¹⁵² C. Fernandez Madrazo,¹⁵² E. Fontanesi,¹⁵² J. Fulcher,¹⁵²
 F. Golf,¹⁵² S. Jeon,¹⁵² J. O’Cain,¹⁵² I. Reed,¹⁵² J. Rohlf,¹⁵² K. Salyer,¹⁵² D. Sperka,¹⁵² D. Spitzbart,¹⁵²
 I. Suarez,¹⁵² A. Tsatsos,¹⁵² E. Wurtz,¹⁵² A. G. Zecchinelli,¹⁵² G. Barone,¹⁵³ G. Benelli,¹⁵³ D. Cutts,¹⁵³
 S. Ellis,¹⁵³ L. Gouskos,¹⁵³ M. Hadley,¹⁵³ U. Heintz,¹⁵³ K. W. Ho,¹⁵³ T. Kwon,¹⁵³ L. Lambrecht,¹⁵³
 G. Landsberg,¹⁵³ K. T. Lau,¹⁵³ J. Luo,¹⁵³ S. Mondal,¹⁵³ J. Roloff,¹⁵³ T. Russell,¹⁵³ S. Sagir,^{153,dddd} X. Shen,¹⁵³
 M. Stamenkovic,¹⁵³ N. Venkatasubramanian,¹⁵³ S. Abbott,¹⁵⁴ B. Barton,¹⁵⁴ R. Breedon,¹⁵⁴ H. Cai,¹⁵⁴
 M. Calderon De La Barca Sanchez,¹⁵⁴ E. Cannata,¹⁵⁴ M. Chertok,¹⁵⁴ M. Citron,¹⁵⁴ J. Conway,¹⁵⁴ P. T. Cox,¹⁵⁴
 R. Erbacher,¹⁵⁴ O. Kukral,¹⁵⁴ G. Mocellin,¹⁵⁴ S. Ostrom,¹⁵⁴ I. Salazar Segovia,¹⁵⁴ J. S. Tafoya Vargas,¹⁵⁴
 W. Wei,¹⁵⁴ S. Yoo,¹⁵⁴ K. Adamidis,¹⁵⁵ M. Bachtis,¹⁵⁵ D. Campos,¹⁵⁵ R. Cousins,¹⁵⁵ A. Datta,¹⁵⁵
 G. Flores Avila,¹⁵⁵ J. Hauser,¹⁵⁵ M. Ignatenko,¹⁵⁵ M. A. Iqbal,¹⁵⁵ T. Lam,¹⁵⁵ Y. f. Lo,¹⁵⁵ E. Manca,¹⁵⁵
 A. Nunez Del Prado,¹⁵⁵ D. Saltzberg,¹⁵⁵ V. Valuev,¹⁵⁵ R. Clare,¹⁵⁶ J. W. Gary,¹⁵⁶ G. Hanson,¹⁵⁶ A. Aportela,¹⁵⁷
 A. Arora,¹⁵⁷ J. G. Branson,¹⁵⁷ S. Cittolin,¹⁵⁷ S. Cooperstein,¹⁵⁷ B. D’Anzi,¹⁵⁷ D. Diaz,¹⁵⁷ J. Duarte,¹⁵⁷
 L. Giannini,¹⁵⁷ Y. Gu,¹⁵⁷ J. Guiang,¹⁵⁷ V. Krutelyov,¹⁵⁷ R. Lee,¹⁵⁷ J. Letts,¹⁵⁷ H. Li,¹⁵⁷ M. Masciovecchio,¹⁵⁷
 F. Mokhtar,¹⁵⁷ S. Mukherjee,¹⁵⁷ M. Pieri,¹⁵⁷ D. Primosch,¹⁵⁷ M. Quinnan,¹⁵⁷ V. Sharma,¹⁵⁷ M. Tadel,¹⁵⁷
 E. Vourliotis,¹⁵⁷ F. Würthwein,¹⁵⁷ A. Yagil,¹⁵⁷ Z. Zhao,¹⁵⁷ A. Barzdukas,¹⁵⁸ L. Brennan,¹⁵⁸ C. Campagnari,¹⁵⁸
 S. Carron Montero,^{158,eeee} K. Downham,¹⁵⁸ C. Grieco,¹⁵⁸ M. M. Hussain,¹⁵⁸ J. Incandela,¹⁵⁸ M. W. K. Lai,¹⁵⁸
 A. J. Li,¹⁵⁸ P. Masterson,¹⁵⁸ J. Richman,¹⁵⁸ S. N. Santpur,¹⁵⁸ U. Sarica,¹⁵⁸ R. Schmitz,¹⁵⁸ F. Setti,¹⁵⁸
 J. Sheplock,¹⁵⁸ D. Stuart,¹⁵⁸ T. Á. Vámi,¹⁵⁸ X. Yan,¹⁵⁸ D. Zhang,¹⁵⁸ A. Albert,¹⁵⁹ S. Bhattacharya,¹⁵⁹
 A. Bornheim,¹⁵⁹ O. Cerri,¹⁵⁹ R. Kansal,¹⁵⁹ J. Mao,¹⁵⁹ H. B. Newman,¹⁵⁹ G. Reales Gutiérrez,¹⁵⁹ T. Sievert,¹⁵⁹
 M. Spiropulu,¹⁵⁹ J. R. Vlimant,¹⁵⁹ R. A. Wynne,¹⁵⁹ S. Xie,¹⁵⁹ J. Alison,¹⁶⁰ S. An,¹⁶⁰ M. Cremonesi,¹⁶⁰
 V. Dutta,¹⁶⁰ E. Y. Ertorer,¹⁶⁰ T. Ferguson,¹⁶⁰ T. A. Gómez Espinosa,¹⁶⁰ A. Harilal,¹⁶⁰ A. Kallil Tharayil,¹⁶⁰
 M. Kanemura,¹⁶⁰ C. Liu,¹⁶⁰ P. Meiring,¹⁶⁰ T. Mudholkar,¹⁶⁰ S. Murthy,¹⁶⁰ P. Palit,¹⁶⁰ K. Park,¹⁶⁰ M. Paulini,¹⁶⁰
 A. Roberts,¹⁶⁰ A. Sanchez,¹⁶⁰ W. Terrill,¹⁶⁰ J. P. Cumalat,¹⁶¹ W. T. Ford,¹⁶¹ A. Hart,¹⁶¹ S. Kwan,¹⁶¹
 J. Parkes,¹⁶¹ C. Savard,¹⁶¹ N. Schonbeck,¹⁶¹ K. Stenson,¹⁶¹ K. A. Ulmer,¹⁶¹ S. R. Wagner,¹⁶¹ N. Zipper,¹⁶¹
 D. Zuolo,¹⁶¹ J. Alexander,¹⁶² X. Chen,¹⁶² J. Dickinson,¹⁶² A. Duquette,¹⁶² J. Fan,¹⁶² X. Fan,¹⁶² J. Grassi,¹⁶²
 S. Hogan,¹⁶² P. Kotamnives,¹⁶² J. Monroy,¹⁶² G. Niendorf,¹⁶² M. Oshiro,¹⁶² J. R. Patterson,¹⁶² A. Ryd,¹⁶²
 J. Thom,¹⁶² P. Wittich,¹⁶² R. Zou,¹⁶² L. Zygala,¹⁶² M. Albrow,¹⁶³ M. Alyari,¹⁶³ O. Amram,¹⁶³ G. Apollinari,¹⁶³
 A. Apresyan,¹⁶³ L. A. T. Bauerdick,¹⁶³ D. Berry,¹⁶³ J. Berryhill,¹⁶³ P. C. Bhat,¹⁶³ K. Burkett,¹⁶³ J. N. Butler,¹⁶³
 A. Canepa,¹⁶³ G. B. Cerati,¹⁶³ H. W. K. Cheung,¹⁶³ F. Chlebana,¹⁶³ C. Cosby,¹⁶³ G. Cummings,¹⁶³ I. Dutta,¹⁶³
 V. D. Elvira,¹⁶³ J. Freeman,¹⁶³ A. Gandrakota,¹⁶³ Z. Gece,¹⁶³ L. Gray,¹⁶³ D. Green,¹⁶³ A. Grummer,¹⁶³
 S. Grünendahl,¹⁶³ D. Guerrero,¹⁶³ O. Gutsche,¹⁶³ R. M. Harris,¹⁶³ T. C. Herwig,¹⁶³ J. Hirschauer,¹⁶³
 V. Innocente,¹⁶³ B. Jayatilaka,¹⁶³ S. Jindariani,¹⁶³ M. Johnson,¹⁶³ U. Joshi,¹⁶³ T. Klijsma,¹⁶³ B. Klima,¹⁶³
 K. H. M. Kwok,¹⁶³ S. Lammel,¹⁶³ C. Lee,¹⁶³ D. Lincoln,¹⁶³ R. Lipton,¹⁶³ T. Liu,¹⁶³ K. Maeshima,¹⁶³
 D. Mason,¹⁶³ P. McBride,¹⁶³ P. Merkel,¹⁶³ S. Mrenna,¹⁶³ S. Nahn,¹⁶³ J. Ngadiuba,¹⁶³ D. Noonan,¹⁶³
 S. Norberg,¹⁶³ V. Papadimitriou,¹⁶³ N. Pastika,¹⁶³ K. Pedro,¹⁶³ C. Pena,^{163,ffff} C. E. Perez Lara,¹⁶³ F. Ravera,¹⁶³
 A. Reinsvold Hall,^{163,gggg} L. Ristori,¹⁶³ M. Safdari,¹⁶³ E. Sexton-Kennedy,¹⁶³ N. Smith,¹⁶³ A. Soha,¹⁶³
 L. Spiegel,¹⁶³ S. Stoynev,¹⁶³ J. Strait,¹⁶³ L. Taylor,¹⁶³ S. Tkaczyk,¹⁶³ N. V. Tran,¹⁶³ L. Uplegger,¹⁶³
 E. W. Vaandering,¹⁶³ C. Wang,¹⁶³ I. Zoi,¹⁶³ C. Aruta,¹⁶⁴ P. Avery,¹⁶⁴ D. Bourilkov,¹⁶⁴ P. Chang,¹⁶⁴
 V. Cherepanov,¹⁶⁴ R. D. Field,¹⁶⁴ C. Huh,¹⁶⁴ E. Koenig,¹⁶⁴ M. Kolosova,¹⁶⁴ J. Konigsberg,¹⁶⁴ A. Korytov,¹⁶⁴
 N. Menendez,¹⁶⁴ G. Mitselmakher,¹⁶⁴ K. Mohrman,¹⁶⁴ A. Muthirakalayil Madhu,¹⁶⁴ N. Rawal,¹⁶⁴
 S. Rosenzweig,¹⁶⁴ V. Sulimov,¹⁶⁴ Y. Takahashi,¹⁶⁴ J. Wang,¹⁶⁴ T. Adams,¹⁶⁵ A. Al Kadhimi,¹⁶⁵ A. Askew,¹⁶⁵
 S. Bower,¹⁶⁵ R. Goff,¹⁶⁵ R. Hashmi,¹⁶⁵ A. Hassani,¹⁶⁵ R. S. Kim,¹⁶⁵ T. Kolberg,¹⁶⁵ G. Martinez,¹⁶⁵ M. Mazza,¹⁶⁵
 H. Prosper,¹⁶⁵ P. R. Prova,¹⁶⁵ R. Yohay,¹⁶⁵ B. Alsufyani,¹⁶⁶ S. Butalla,¹⁶⁶ S. Das,¹⁶⁶ M. Hohmann,¹⁶⁶
 M. Lavinsky,¹⁶⁶ E. Yanes,¹⁶⁶ M. R. Adams,¹⁶⁷ N. Barnett,¹⁶⁷ A. Baty,¹⁶⁷ C. Bennett,¹⁶⁷ R. Cavanaugh,¹⁶⁷
 R. Escobar Franco,¹⁶⁷ O. Evdokimov,¹⁶⁷ C. E. Gerber,¹⁶⁷ H. Gupta,¹⁶⁷ M. Hawksworth,¹⁶⁷ A. Hingrajiya,¹⁶⁷
 D. J. Hofman,¹⁶⁷ J. h. Lee,¹⁶⁷ C. Mills,¹⁶⁷ S. Nanda,¹⁶⁷ G. Nigmatkulov,¹⁶⁷ B. Ozek,¹⁶⁷ T. Phan,¹⁶⁷
 D. Pilipovic,¹⁶⁷ R. Pradhan,¹⁶⁷ E. Prifti,¹⁶⁷ P. Roy,¹⁶⁷ T. Roy,¹⁶⁷ N. Singh,¹⁶⁷ M. B. Tonjes,¹⁶⁷ N. Varelas,¹⁶⁷
 M. A. Wadud,¹⁶⁷ J. Yoo,¹⁶⁷ M. Alhousseini,¹⁶⁸ D. Blend,¹⁶⁸ K. Dilsiz,^{168,hhhh} O. K. Köseyan,¹⁶⁸

A. Mestvirishvili^{168,iiii} O. Neogi,¹⁶⁸ H. Ogul^{168,jjjj} Y. Onel¹⁶⁸ A. Penzo¹⁶⁸ C. Snyder,¹⁶⁸ E. Tiras^{168,kkkk}
 B. Blumenfeld¹⁶⁹ J. Davis¹⁶⁹ A. V. Gritsan¹⁶⁹ L. Kang¹⁶⁹ S. Kyriacou¹⁶⁹ P. Maksimovic¹⁶⁹ M. Roguljic¹⁶⁹
 S. Sekhar¹⁶⁹ M. V. Srivastav¹⁶⁹ M. Swartz¹⁶⁹ A. Abreu¹⁷⁰ L. F. Alcerro Alcerro¹⁷⁰ J. Anguiano¹⁷⁰
 S. Arteaga Escatel¹⁷⁰ P. Baringer¹⁷⁰ A. Bean¹⁷⁰ Z. Flowers¹⁷⁰ D. Grove¹⁷⁰ J. King¹⁷⁰ G. Krintiras¹⁷⁰
 M. Lazarovits¹⁷⁰ C. Le Mahieu¹⁷⁰ J. Marquez¹⁷⁰ M. Murray¹⁷⁰ M. Nickel¹⁷⁰ S. Popescu^{170,llll} C. Rogan¹⁷⁰
 C. Royon¹⁷⁰ S. Rudrabhatla¹⁷⁰ S. Sanders¹⁷⁰ C. Smith¹⁷⁰ G. Wilson¹⁷⁰ B. Allmond¹⁷¹ N. Islam,¹⁷¹
 A. Ivanov¹⁷¹ K. Kaadze¹⁷¹ Y. Maravin¹⁷¹ J. Natoli¹⁷¹ G. G. Reddy¹⁷¹ D. Roy¹⁷¹ G. Sorrentino¹⁷¹
 A. Baden¹⁷² A. Belloni¹⁷² J. Bistany-riebman,¹⁷² S. C. Eno¹⁷² N. J. Hadley¹⁷² S. Jabeen¹⁷² R. G. Kellogg¹⁷²
 T. Koeth¹⁷² B. Kronheim,¹⁷² S. Lascio¹⁷² P. Major¹⁷² A. C. Mignerey¹⁷² C. Palmer¹⁷² C. Papageorgakis¹⁷²
 M. M. Paranje,¹⁷² E. Popova^{172,mmmm} A. Shevelev¹⁷² L. Zhang¹⁷² C. Baldenegro Barrera¹⁷³ H. Bossi¹⁷³
 S. Bright-Thonney¹⁷³ I. A. Cali¹⁷³ Y. c. Chen¹⁷³ P. c. Chou¹⁷³ M. D'Alfonso¹⁷³ J. Eysermans¹⁷³ C. Freer¹⁷³
 G. Gomez-Ceballos¹⁷³ M. Goncharov,¹⁷³ G. Grosso¹⁷³ P. Harris,¹⁷³ D. Hoang¹⁷³ G. M. Innocenti¹⁷³
 D. Kovalskiy¹⁷³ J. Krupa¹⁷³ L. Lavezzo¹⁷³ Y.-J. Lee¹⁷³ K. Long¹⁷³ C. McGinn¹⁷³ A. Novak¹⁷³
 M. I. Park¹⁷³ C. Paus¹⁷³ C. Reissel¹⁷³ C. Roland¹⁷³ G. Roland¹⁷³ S. Rothman¹⁷³ T. a. Sheng¹⁷³
 G. S. F. Stephans¹⁷³ D. Walter¹⁷³ Z. Wang¹⁷³ B. Wyslouch¹⁷³ T. J. Yang¹⁷³ B. Crossman¹⁷⁴ W. J. Jackson,¹⁷⁴
 C. Kapsiak¹⁷⁴ M. Krohn¹⁷⁴ D. Mahon¹⁷⁴ J. Mans¹⁷⁴ B. Marzocchi¹⁷⁴ R. Rusack¹⁷⁴ O. Sancar¹⁷⁴
 R. Saradhy¹⁷⁴ N. Strobbe¹⁷⁴ K. Bloom¹⁷⁵ D. R. Claes¹⁷⁵ G. Haza¹⁷⁵ J. Hossain¹⁷⁵ C. Joo¹⁷⁵
 I. Kravchenko¹⁷⁵ A. Rohilla¹⁷⁵ J. E. Siado¹⁷⁵ W. Tabb¹⁷⁵ A. Vagnerini¹⁷⁵ A. Wightman¹⁷⁵ F. Yan¹⁷⁵
 H. Bandyopadhyay¹⁷⁶ L. Hay¹⁷⁶ H. w. Hsia¹⁷⁶ I. Iashvili¹⁷⁶ A. Kalogeropoulos¹⁷⁶ A. Kharchilava¹⁷⁶
 A. Mandal¹⁷⁶ M. Morris¹⁷⁶ D. Nguyen¹⁷⁶ S. Rappoccio¹⁷⁶ H. Rejeb Sfar,¹⁷⁶ A. Williams¹⁷⁶ P. Young¹⁷⁶
 D. Yu¹⁷⁶ G. Alverson¹⁷⁷ E. Barberis¹⁷⁷ J. Bonilla¹⁷⁷ B. Bylsma,¹⁷⁷ M. Campana¹⁷⁷ J. Dervan¹⁷⁷
 Y. Haddad¹⁷⁷ Y. Han¹⁷⁷ I. Israr¹⁷⁷ A. Krishna¹⁷⁷ M. Lu¹⁷⁷ N. Manganelli¹⁷⁷ R. Mccarthy¹⁷⁷
 D. M. Morse¹⁷⁷ T. Orimoto¹⁷⁷ L. Skinnari¹⁷⁷ C. S. Thoreson¹⁷⁷ E. Tsai¹⁷⁷ D. Wood¹⁷⁷ S. Dittmer¹⁷⁸
 K. A. Hahn¹⁷⁸ Y. Liu¹⁷⁸ M. McGinnis¹⁷⁸ Y. Miao¹⁷⁸ D. G. Monk¹⁷⁸ M. H. Schmitt¹⁷⁸ A. Taliercio¹⁷⁸
 M. Velasco¹⁷⁸ J. Wang,¹⁷⁸ G. Agarwal,¹⁷⁹ R. Band¹⁷⁹ R. Bucci,¹⁷⁹ S. Castells¹⁷⁹ A. Das¹⁷⁹ A. Ehnis,¹⁷⁹
 R. Goldouzian¹⁷⁹ M. Hildreth¹⁷⁹ K. Hurtado Anampa¹⁷⁹ T. Ivanov¹⁷⁹ C. Jessop¹⁷⁹ A. Karneyeu¹⁷⁹
 K. Lannon¹⁷⁹ J. Lawrence¹⁷⁹ N. Loukas¹⁷⁹ L. Lutton¹⁷⁹ J. Mariano¹⁷⁹ N. Marinelli,¹⁷⁹ I. Mcalister,¹⁷⁹
 T. McCauley¹⁷⁹ C. Mcgrady¹⁷⁹ C. Moore¹⁷⁹ Y. Musienko^{179,nnnn} H. Nelson¹⁷⁹ M. Osherson¹⁷⁹
 A. Piccinelli¹⁷⁹ R. Ruchti¹⁷⁹ A. Townsend¹⁷⁹ Y. Wan,¹⁷⁹ M. Wayne¹⁷⁹ H. Yockey,¹⁷⁹ A. Basnet¹⁸⁰
 M. Carrigan¹⁸⁰ R. De Los Santos¹⁸⁰ L. S. Durkin¹⁸⁰ C. Hill¹⁸⁰ M. Joyce¹⁸⁰ M. Nunez Ornelas¹⁸⁰
 D. A. Wenzl,¹⁸⁰ B. L. Winer¹⁸⁰ B. R. Yates¹⁸⁰ H. Bouchamaoui¹⁸¹ G. Dezoort¹⁸¹ P. Elmer¹⁸¹ A. Frankenthal¹⁸¹
 M. Galli¹⁸¹ B. Greenberg¹⁸¹ N. Haubrich¹⁸¹ K. Kennedy,¹⁸¹ G. Kopp¹⁸¹ Y. Lai¹⁸¹ D. Lange¹⁸¹
 A. Loeliger¹⁸¹ D. Marlow¹⁸¹ I. Ojalvo¹⁸¹ J. Olsen¹⁸¹ F. Simpson¹⁸¹ D. Stickland¹⁸¹ C. Tully¹⁸¹
 S. Malik¹⁸² R. Sharma¹⁸² S. Chandra¹⁸³ R. Chawla¹⁸³ A. Gu¹⁸³ L. Gutay,¹⁸³ M. Jones¹⁸³ A. W. Jung¹⁸³
 D. Kondratyev¹⁸³ M. Liu¹⁸³ G. Negro¹⁸³ N. Neumeister¹⁸³ G. Paspalaki¹⁸³ S. Piperov¹⁸³ N. R. Saha¹⁸³
 J. F. Schulte¹⁸³ F. Wang¹⁸³ A. Wildridge¹⁸³ W. Xie¹⁸³ Y. Yao¹⁸³ Y. Zhong¹⁸³ N. Parashar¹⁸⁴ A. Pathak¹⁸⁴
 E. Shumka¹⁸⁴ D. Acosta¹⁸⁵ A. Agrawal¹⁸⁵ C. Arbour¹⁸⁵ T. Carnahan¹⁸⁵ P. Das¹⁸⁵ K. M. Ecklund¹⁸⁵
 S. Freed¹⁸⁵ P. Gardner,¹⁸⁵ F. J. M. Geurts¹⁸⁵ T. Huang¹⁸⁵ I. Krommydas¹⁸⁵ N. Lewis,¹⁸⁵ W. Li¹⁸⁵ J. Lin¹⁸⁵
 O. Miguel Colin¹⁸⁵ B. P. Padley¹⁸⁵ R. Redjimi¹⁸⁵ J. Rotter¹⁸⁵ M. Wulansatiti¹⁸⁵ E. Yigitbasi¹⁸⁵ Y. Zhang¹⁸⁵
 O. Bessidskaia Bylund,¹⁸⁶ A. Bodek¹⁸⁶ P. de Barbaro^{186,a} R. Demina¹⁸⁶ A. Garcia-Bellido¹⁸⁶ H. S. Hare¹⁸⁶
 O. Hindrichs¹⁸⁶ N. Parmar¹⁸⁶ P. Parygin^{186,nnnn} H. Seo¹⁸⁶ R. Taus¹⁸⁶ B. Chiarito,¹⁸⁷ J. P. Chou¹⁸⁷
 S. V. Clark¹⁸⁷ S. Donnelly,¹⁸⁷ D. Gadkari¹⁸⁷ Y. Gershtein¹⁸⁷ E. Halkiadakis¹⁸⁷ C. Houghton¹⁸⁷
 D. Jaroslawski¹⁸⁷ A. Kobert¹⁸⁷ S. Konstantinou¹⁸⁷ I. Laflotte¹⁸⁷ A. Lath¹⁸⁷ J. Martins¹⁸⁷ M. Perez Prada¹⁸⁷
 B. Rand¹⁸⁷ J. Reichert¹⁸⁷ P. Saha¹⁸⁷ S. Salur¹⁸⁷ S. Schnetzer,¹⁸⁷ S. Somalwar¹⁸⁷ R. Stone¹⁸⁷ S. A. Thayil¹⁸⁷
 S. Thomas,¹⁸⁷ J. Vora¹⁸⁷ D. Ally¹⁸⁸ A. G. Delannoy¹⁸⁸ S. Fiorendi¹⁸⁸ J. Harris,¹⁸⁸ T. Holmes¹⁸⁸
 A. R. Kanuganti¹⁸⁸ N. Karunarathna¹⁸⁸ J. Lawless,¹⁸⁸ L. Lee¹⁸⁸ E. Nibigira¹⁸⁸ B. Skipworth,¹⁸⁸ S. Spanier¹⁸⁸
 D. Aebi¹⁸⁹ M. Ahmad¹⁸⁹ T. Akhter¹⁸⁹ K. Androsov¹⁸⁹ A. Bolshov,¹⁸⁹ O. Bouhali^{189,nnnn} A. Cagnotta¹⁸⁹
 V. D'Amante¹⁸⁹ R. Eusebi¹⁸⁹ P. Flanagan¹⁸⁹ J. Gilmore¹⁸⁹ Y. Guo,¹⁸⁹ T. Kamon¹⁸⁹ S. Luo¹⁸⁹ R. Mueller¹⁸⁹
 A. Safonov¹⁸⁹ N. Akchurin¹⁹⁰ J. Damgov¹⁹⁰ Y. Feng¹⁹⁰ N. Gogate¹⁹⁰ Y. Kazhykarim,¹⁹⁰ K. Lamichhane¹⁹⁰

S. W. Lee¹⁹⁰, C. Madrid¹⁹⁰, A. Mankel¹⁹⁰, T. Peltola¹⁹⁰, I. Volobouev¹⁹⁰, E. Appelt¹⁹¹, Y. Chen¹⁹¹, S. Greene¹⁹¹,
 A. Gurrola¹⁹¹, W. Johns¹⁹¹, R. Kunnawalkam Elayavalli¹⁹¹, A. Melo¹⁹¹, D. Rathjens¹⁹¹, F. Romeo¹⁹¹,
 P. Sheldon¹⁹¹, S. Tuo¹⁹¹, J. Velkovska¹⁹¹, J. Viinikainen¹⁹¹, J. Zhang¹⁹¹, B. Cardwell¹⁹², H. Chung¹⁹², B. Cox¹⁹²,
 J. Hakala¹⁹², G. Hamilton Ilha Machado¹⁹², R. Hirosky¹⁹², M. Jose¹⁹², A. Ledovsky¹⁹², C. Mantilla¹⁹², C. Neu¹⁹²,
 C. Ramón Álvarez¹⁹², Z. Wu¹⁹², S. Bhattacharya¹⁹³, P. E. Karchin¹⁹³, A. Aravind¹⁹⁴, S. Banerjee¹⁹⁴, K. Black¹⁹⁴,
 T. Bose¹⁹⁴, E. Chavez¹⁹⁴, S. Dasu¹⁹⁴, P. Everaerts¹⁹⁴, C. Galloni¹⁹⁴, H. He¹⁹⁴, M. Herndon¹⁹⁴, A. Herve¹⁹⁴,
 C. K. Koraka¹⁹⁴, S. Lomte¹⁹⁴, R. Loveless¹⁹⁴, A. Mallampalli¹⁹⁴, A. Mohammadi¹⁹⁴, S. Mondal¹⁹⁴, T. Nelson¹⁹⁴,
 G. Parida¹⁹⁴, L. Pétrec¹⁹⁴, D. Pinna¹⁹⁴, A. Savin¹⁹⁴, V. Shang¹⁹⁴, V. Sharma¹⁹⁴, W. H. Smith¹⁹⁴, D. Teague¹⁹⁴,
 H. F. Tsoi¹⁹⁴, W. Vetens¹⁹⁴, A. Warden¹⁹⁴, S. Afanasiev¹⁹⁵, V. Alexakhin¹⁹⁵, Yu. Andreev¹⁹⁵, T. Aushev¹⁹⁵,
 D. Budkouski¹⁹⁵, R. Chistov¹⁹⁵, M. Danilov¹⁹⁵, T. Dimova¹⁹⁵, A. Ershov¹⁹⁵, S. Gninenko¹⁹⁵, I. Gorbunov¹⁹⁵,
 A. Gribushin¹⁹⁵, A. Kamenev¹⁹⁵, V. Karjavine¹⁹⁵, M. Kirsanov¹⁹⁵, V. Klyukhin¹⁹⁵, O. Kodolova^{195,0000},
 V. Korenkov¹⁹⁵, I. Korsakov¹⁹⁵, A. Kozyrev¹⁹⁵, N. Krasnikov¹⁹⁵, A. Lanev¹⁹⁵, A. Malakhov¹⁹⁵, V. Matveev¹⁹⁵,
 A. Nikitenko^{195,pppp,0000}, V. Palichik¹⁹⁵, V. Perelygin¹⁹⁵, S. Petrushanko¹⁹⁵, S. Polikarpov¹⁹⁵, O. Radchenko¹⁹⁵,
 M. Savina¹⁹⁵, V. Shalaev¹⁹⁵, S. Shmatov¹⁹⁵, S. Shulha¹⁹⁵, Y. Skovpen¹⁹⁵, K. Slizhevskiy¹⁹⁵, V. Smirnov¹⁹⁵,
 O. Teryaev¹⁹⁵, I. Tlisova¹⁹⁵, A. Toropin¹⁹⁵, N. Voytishin¹⁹⁵, A. Zarubin¹⁹⁵, I. Zhizhin¹⁹⁵, L. Dudko¹⁹⁶,
 K. Ivanov¹⁹⁶, V. Kim^{196,mmmm}, V. Murzin¹⁹⁶, V. Oreshkin¹⁹⁶, D. Sosnov¹⁹⁶, E. Boos¹⁹⁶, V. Bunichev¹⁹⁶,
 M. Dubinin^{196,ffff}, V. Savrin¹⁹⁶, and A. Snigirev¹⁹⁶

(CMS Collaboration)

¹*Yerevan Physics Institute, Yerevan, Armenia*

²*Institut für Hochenergiephysik, Vienna, Austria*

³*Universiteit Antwerpen, Antwerpen, Belgium*

⁴*Vrije Universiteit Brussel, Brussel, Belgium*

⁵*Université Libre de Bruxelles, Bruxelles, Belgium*

⁶*Ghent University, Ghent, Belgium*

⁷*Université Catholique de Louvain, Louvain-la-Neuve, Belgium*

⁸*Centro Brasileiro de Pesquisas Físicas, Rio de Janeiro, Brazil*

⁹*Universidade do Estado do Rio de Janeiro, Rio de Janeiro, Brazil*

¹⁰*Universidade Estadual Paulista, Universidade Federal do ABC, São Paulo, Brazil*

¹¹*Institute for Nuclear Research and Nuclear Energy, Bulgarian Academy of Sciences, Sofia, Bulgaria*

¹²*University of Sofia, Sofia, Bulgaria*

¹³*Instituto De Alta Investigación, Universidad de Tarapacá, Casilla 7 D, Arica, Chile*

¹⁴*Universidad Tecnica Federico Santa Maria, Valparaiso, Chile*

¹⁵*Beihang University, Beijing, China*

¹⁶*Department of Physics, Tsinghua University, Beijing, China*

¹⁷*Institute of High Energy Physics, Beijing, China*

¹⁸*State Key Laboratory of Nuclear Physics and Technology, Peking University, Beijing, China*

¹⁹*State Key Laboratory of Nuclear Physics and Technology, Institute of Quantum Matter,*

South China Normal University, Guangzhou, China

²⁰*Sun Yat-Sen University, Guangzhou, China*

²¹*University of Science and Technology of China, Hefei, China*

²²*Nanjing Normal University, Nanjing, China*

²³*Institute of Modern Physics and Key Laboratory of Nuclear Physics and Ion-beam Application (MOE)—*

Fudan University, Shanghai, China

²⁴*Zhejiang University, Hangzhou, Zhejiang, China*

²⁵*Universidad de Los Andes, Bogota, Colombia*

²⁶*Universidad de Antioquia, Medellin, Colombia*

²⁷*University of Split, Faculty of Electrical Engineering, Mechanical Engineering and Naval Architecture,*
Split, Croatia

²⁸*University of Split, Faculty of Science, Split, Croatia*

²⁹*Institute Rudjer Boskovic, Zagreb, Croatia*

³⁰*University of Cyprus, Nicosia, Cyprus*

³¹*Charles University, Prague, Czech Republic*

³²*Escuela Politecnica Nacional, Quito, Ecuador*

³³*Universidad San Francisco de Quito, Quito, Ecuador*

- ³⁴*Academy of Scientific Research and Technology of the Arab Republic of Egypt, Egyptian Network of High Energy Physics, Cairo, Egypt*
- ³⁵*Center for High Energy Physics (CHEP-FU), Fayoum University, El-Fayoum, Egypt*
- ³⁶*National Institute of Chemical Physics and Biophysics, Tallinn, Estonia*
- ³⁷*Department of Physics, University of Helsinki, Helsinki, Finland*
- ³⁸*Helsinki Institute of Physics, Helsinki, Finland*
- ³⁹*Lappeenranta-Lahti University of Technology, Lappeenranta, Finland*
- ⁴⁰*IRFU, CEA, Université Paris-Saclay, Gif-sur-Yvette, France*
- ⁴¹*Laboratoire Leprince-Ringuet, CNRS/IN2P3, Ecole Polytechnique, Institut Polytechnique de Paris, Palaiseau, France*
- ⁴²*Université de Strasbourg, CNRS, IPHC UMR 7178, Strasbourg, France*
- ⁴³*Centre de Calcul de l'Institut National de Physique Nucleaire et de Physique des Particules, CNRS/IN2P3, Villeurbanne, France*
- ⁴⁴*Institut de Physique des 2 Infinis de Lyon (IP2I), Villeurbanne, France*
- ⁴⁵*Georgian Technical University, Tbilisi, Georgia*
- ⁴⁶*RWTH Aachen University, I. Physikalisches Institut, Aachen, Germany*
- ⁴⁷*RWTH Aachen University, III. Physikalisches Institut A, Aachen, Germany*
- ⁴⁸*RWTH Aachen University, III. Physikalisches Institut B, Aachen, Germany*
- ⁴⁹*Deutsches Elektronen-Synchrotron, Hamburg, Germany*
- ⁵⁰*University of Hamburg, Hamburg, Germany*
- ⁵¹*Karlsruher Institut fuer Technologie, Karlsruhe, Germany*
- ⁵²*Institute of Nuclear and Particle Physics (INPP), NCSR Demokritos, Aghia Paraskevi, Greece*
- ⁵³*National and Kapodistrian University of Athens, Athens, Greece*
- ⁵⁴*National Technical University of Athens, Athens, Greece*
- ⁵⁵*University of Ioánnina, Ioánnina, Greece*
- ⁵⁶*HUN-REN Wigner Research Centre for Physics, Budapest, Hungary*
- ⁵⁷*MTA-ELTE Lendület CMS Particle and Nuclear Physics Group, Eötvös Loránd University, Budapest, Hungary*
- ⁵⁸*Faculty of Informatics, University of Debrecen, Debrecen, Hungary*
- ⁵⁹*HUN-REN ATOMKI—Institute of Nuclear Research, Debrecen, Hungary*
- ⁶⁰*Karoly Robert Campus, MATE Institute of Technology, Gyongyos, Hungary*
- ⁶¹*Panjab University, Chandigarh, India*
- ⁶²*University of Delhi, Delhi, India*
- ⁶³*University of Hyderabad, Hyderabad, India*
- ⁶⁴*Indian Institute of Technology Kanpur, Kanpur, India*
- ⁶⁵*Saha Institute of Nuclear Physics, HBNI, Kolkata, India*
- ⁶⁶*Indian Institute of Technology Madras, Madras, India*
- ⁶⁷*IISER Mohali, India, Mohali, India*
- ⁶⁸*Tata Institute of Fundamental Research-A, Mumbai, India*
- ⁶⁹*Tata Institute of Fundamental Research-B, Mumbai, India*
- ⁷⁰*National Institute of Science Education and Research, An OCC of Homi Bhabha National Institute, Bhubaneswar, Odisha, India*
- ⁷¹*Indian Institute of Science Education and Research (IISER), Pune, India*
- ⁷²*Indian Institute of Technology Hyderabad, Telangana, India*
- ⁷³*Isfahan University of Technology, Isfahan, Iran*
- ⁷⁴*Institute for Research in Fundamental Sciences (IPM), Tehran, Iran*
- ⁷⁵*University College Dublin, Dublin, Ireland*
- ^{76a}*INFN Sezione di Bari, Bari, Italy*
- ^{76b}*Università di Bari, Bari, Italy*
- ^{76c}*Politecnico di Bari, Bari, Italy*
- ^{77a}*INFN Sezione di Bologna, Bologna, Italy*
- ^{77b}*Università di Bologna, Bologna, Italy*
- ^{78a}*INFN Sezione di Catania, Catania, Italy*
- ^{78b}*Università di Catania, Catania, Italy*
- ^{79a}*INFN Sezione di Firenze, Firenze, Italy*
- ^{79b}*Università di Firenze, Firenze, Italy*
- ⁸⁰*INFN Laboratori Nazionali di Frascati, Frascati, Italy*
- ^{81a}*INFN Sezione di Genova, Genova, Italy*
- ^{81b}*Università di Genova, Genova, Italy*

- ^{82a}*INFN Sezione di Milano-Bicocca, Milano, Italy*
^{82b}*Università di Milano-Bicocca, Milano, Italy*
^{83a}*INFN Sezione di Napoli, Napoli, Italy*
^{83b}*Università di Napoli 'Federico II', Napoli, Italy*
^{83c}*Università della Basilicata, Potenza, Italy*
^{83d}*Scuola Superiore Meridionale (SSM), Napoli, Italy*
^{84a}*INFN Sezione di Padova, Padova, Italy*
^{84b}*Università di Padova, Padova, Italy*
^{84c}*Università degli Studi di Cagliari, Cagliari, Italy*
^{85a}*INFN Sezione di Pavia, Pavia, Italy*
^{85b}*Università di Pavia, Pavia, Italy*
^{86a}*INFN Sezione di Perugia, Perugia, Italy*
^{86b}*Università di Perugia, Perugia, Italy*
^{87a}*INFN Sezione di Pisa, Pisa, Italy*
^{87b}*Università di Pisa, Pisa, Italy*
^{87c}*Scuola Normale Superiore di Pisa, Pisa, Italy*
^{87d}*Università di Siena, Siena, Italy*
^{88a}*INFN Sezione di Roma, Roma, Italy*
^{88b}*Sapienza Università di Roma, Roma, Italy*
^{89a}*INFN Sezione di Torino, Torino, Italy*
^{89b}*Università di Torino, Torino, Italy*
^{89c}*Università del Piemonte Orientale, Novara, Italy*
^{90a}*INFN Sezione di Trieste, Trieste, Italy*
^{90b}*Università di Trieste, Trieste, Italy*
⁹¹*Kyungpook National University, Daegu, Korea*
⁹²*Department of Mathematics and Physics—GWNu, Gangneung, Korea*
⁹³*Chonnam National University, Institute for Universe and Elementary Particles, Kwangju, Korea*
⁹⁴*Hanyang University, Seoul, Korea*
⁹⁵*Korea University, Seoul, Korea*
⁹⁶*Kyung Hee University, Department of Physics, Seoul, Korea*
⁹⁷*Sejong University, Seoul, Korea*
⁹⁸*Seoul National University, Seoul, Korea*
⁹⁹*University of Seoul, Seoul, Korea*
¹⁰⁰*Yonsei University, Department of Physics, Seoul, Korea*
¹⁰¹*Sungkyunkwan University, Suwon, Korea*
¹⁰²*College of Engineering and Technology, American University of the Middle East (AUM),
Dasman, Kuwait*
¹⁰³*Kuwait University—College of Science—Department of Physics, Safat, Kuwait*
¹⁰⁴*Riga Technical University, Riga, Latvia*
¹⁰⁵*University of Latvia (LU), Riga, Latvia*
¹⁰⁶*Vilnius University, Vilnius, Lithuania*
¹⁰⁷*National Centre for Particle Physics, Universiti Malaya, Kuala Lumpur, Malaysia*
¹⁰⁸*Universidad de Sonora (UNISON), Hermosillo, Mexico*
¹⁰⁹*Centro de Investigación y de Estudios Avanzados del IPN, Mexico City, Mexico*
¹¹⁰*Universidad Iberoamericana, Mexico City, Mexico*
¹¹¹*Benemerita Universidad Autónoma de Puebla, Puebla, Mexico*
¹¹²*University of Montenegro, Podgorica, Montenegro*
¹¹³*University of Canterbury, Christchurch, New Zealand*
¹¹⁴*National Centre for Physics, Quaid-I-Azam University, Islamabad, Pakistan*
¹¹⁵*AGH University of Krakow, Krakow, Poland*
¹¹⁶*National Centre for Nuclear Research, Swierk, Poland*
¹¹⁷*Institute of Experimental Physics, Faculty of Physics, University of Warsaw, Warsaw, Poland*
¹¹⁸*Warsaw University of Technology, Warsaw, Poland*
¹¹⁹*Laboratório de Instrumentação e Física Experimental de Partículas, Lisboa, Portugal*
¹²⁰*Faculty of Physics, University of Belgrade, Belgrade, Serbia*
¹²¹*VINCA Institute of Nuclear Sciences, University of Belgrade, Belgrade, Serbia*
¹²²*Centro de Investigaciones Energéticas Medioambientales y Tecnológicas (CIEMAT), Madrid, Spain*
¹²³*Universidad Autónoma de Madrid, Madrid, Spain*
¹²⁴*Universidad de Oviedo, Instituto Universitario de Ciencias y Tecnologías Espaciales de Asturias
(ICTEA), Oviedo, Spain*

- ¹²⁵*Instituto de Física de Cantabria (IFCA), CSIC-Universidad de Cantabria, Santander, Spain*
- ¹²⁶*University of Colombo, Colombo, Sri Lanka*
- ¹²⁷*University of Ruhuna, Department of Physics, Matara, Sri Lanka*
- ¹²⁸*CERN, European Organization for Nuclear Research, Geneva, Switzerland*
- ¹²⁹*PSI Center for Neutron and Muon Sciences, Villigen, Switzerland*
- ¹³⁰*ETH Zurich—Institute for Particle Physics and Astrophysics (IPA), Zurich, Switzerland*
- ¹³¹*Universität Zürich, Zurich, Switzerland*
- ¹³²*National Central University, Chung-Li, Taiwan*
- ¹³³*National Taiwan University (NTU), Taipei, Taiwan*
- ¹³⁴*High Energy Physics Research Unit, Department of Physics, Faculty of Science, Chulalongkorn University, Bangkok, Thailand*
- ¹³⁵*Tunis El Manar University, Tunis, Tunisia*
- ¹³⁶*Çukurova University, Physics Department, Science and Art Faculty, Adana, Turkey*
- ¹³⁷*Middle East Technical University, Physics Department, Ankara, Turkey*
- ¹³⁸*Bogazici University, Istanbul, Turkey*
- ¹³⁹*Istanbul Technical University, Istanbul, Turkey*
- ¹⁴⁰*Istanbul University, Istanbul, Turkey*
- ¹⁴¹*Yildiz Technical University, Istanbul, Turkey*
- ¹⁴²*Institute for Scintillation Materials of National Academy of Science of Ukraine, Kharkiv, Ukraine*
- ¹⁴³*National Science Centre, Kharkiv Institute of Physics and Technology, Kharkiv, Ukraine*
- ¹⁴⁴*University of Bristol, Bristol, United Kingdom*
- ¹⁴⁵*Rutherford Appleton Laboratory, Didcot, United Kingdom*
- ¹⁴⁶*Imperial College, London, United Kingdom*
- ¹⁴⁷*Brunel University, Uxbridge, United Kingdom*
- ¹⁴⁸*Baylor University, Waco, Texas, USA*
- ¹⁴⁹*Bethel University, St. Paul, Minnesota, USA*
- ¹⁵⁰*Catholic University of America, Washington, DC, USA*
- ¹⁵¹*The University of Alabama, Tuscaloosa, Alabama, USA*
- ¹⁵²*Boston University, Boston, Massachusetts, USA*
- ¹⁵³*Brown University, Providence, Rhode Island, USA*
- ¹⁵⁴*University of California, Davis, Davis, California, USA*
- ¹⁵⁵*University of California, Los Angeles, California, USA*
- ¹⁵⁶*University of California, Riverside, Riverside, California, USA*
- ¹⁵⁷*University of California, San Diego, La Jolla, California, USA*
- ¹⁵⁸*University of California, Santa Barbara—Department of Physics, Santa Barbara, California, USA*
- ¹⁵⁹*California Institute of Technology, Pasadena, California, USA*
- ¹⁶⁰*Carnegie Mellon University, Pittsburgh, Pennsylvania, USA*
- ¹⁶¹*University of Colorado Boulder, Boulder, Colorado, USA*
- ¹⁶²*Cornell University, Ithaca, New York, USA*
- ¹⁶³*Fermi National Accelerator Laboratory, Batavia, Illinois, USA*
- ¹⁶⁴*University of Florida, Gainesville, Florida, USA*
- ¹⁶⁵*Florida State University, Tallahassee, Florida, USA*
- ¹⁶⁶*Florida Institute of Technology, Melbourne, Florida, USA*
- ¹⁶⁷*University of Illinois Chicago, Chicago, Illinois, USA*
- ¹⁶⁸*The University of Iowa, Iowa City, Iowa, USA*
- ¹⁶⁹*Johns Hopkins University, Baltimore, Maryland, USA*
- ¹⁷⁰*The University of Kansas, Lawrence, Kansas, USA*
- ¹⁷¹*Kansas State University, Manhattan, Kansas, USA*
- ¹⁷²*University of Maryland, College Park, Maryland, USA*
- ¹⁷³*Massachusetts Institute of Technology, Cambridge, Massachusetts, USA*
- ¹⁷⁴*University of Minnesota, Minneapolis, Minnesota, USA*
- ¹⁷⁵*University of Nebraska-Lincoln, Lincoln, Nebraska, USA*
- ¹⁷⁶*State University of New York at Buffalo, Buffalo, New York, USA*
- ¹⁷⁷*Northeastern University, Boston, Massachusetts, USA*
- ¹⁷⁸*Northwestern University, Evanston, Illinois, USA*
- ¹⁷⁹*University of Notre Dame, Notre Dame, Indiana, USA*
- ¹⁸⁰*The Ohio State University, Columbus, Ohio, USA*
- ¹⁸¹*Princeton University, Princeton, New Jersey, USA*
- ¹⁸²*University of Puerto Rico, Mayaguez, Puerto Rico, USA*
- ¹⁸³*Purdue University, West Lafayette, Indiana, USA*

- ¹⁸⁴*Purdue University Northwest, Hammond, Indiana, USA*
¹⁸⁵*Rice University, Houston, Texas, USA*
¹⁸⁶*University of Rochester, Rochester, New York, USA*
¹⁸⁷*Rutgers, The State University of New Jersey, Piscataway, New Jersey, USA*
¹⁸⁸*University of Tennessee, Knoxville, Tennessee, USA*
¹⁸⁹*Texas A&M University, College Station, Texas, USA*
¹⁹⁰*Texas Tech University, Lubbock, Texas, USA*
¹⁹¹*Vanderbilt University, Nashville, Tennessee, USA*
¹⁹²*University of Virginia, Charlottesville, Virginia, USA*
¹⁹³*Wayne State University, Detroit, Michigan, USA*
¹⁹⁴*University of Wisconsin—Madison, Madison, Wisconsin, USA*
¹⁹⁵*An institute or international laboratory covered by a cooperation agreement with CERN*
¹⁹⁶*An institute formerly covered by a cooperation agreement with CERN*

^aDeceased.

^bAlso at Yerevan State University, Yerevan, Armenia.

^cAlso at TU Wien, Vienna, Austria.

^dAlso at Ghent University, Ghent, Belgium.

^eAlso at Universidade do Estado do Rio de Janeiro, Rio de Janeiro, Brazil.

^fAlso at FACAMP—Faculdades de Campinas, Sao Paulo, Brazil.

^gAlso at Universidade Estadual de Campinas, Campinas, Brazil.

^hAlso at Federal University of Rio Grande do Sul, Porto Alegre, Brazil.

ⁱAlso at The University of the State of Amazonas, Manaus, Brazil.

^jAlso at University of Chinese Academy of Sciences, Beijing, China.

^kAlso at China Center of Advanced Science and Technology, Beijing, China.

^lAlso at University of Chinese Academy of Sciences, Beijing, China.

^mAlso at School of Physics, Zhengzhou University, Zhengzhou, China.

ⁿAlso at Henan Normal University, Xinxiang, China.

^oAlso at University of Shanghai for Science and Technology, Shanghai, China.

^pAlso at The University of Iowa, Iowa City, Iowa, USA.

^qAlso at Center for High Energy Physics, Peking University, Beijing, China.

^rAlso at British University in Egypt, Cairo, Egypt.

^sAlso at Cairo University, Cairo, Egypt.

^tAlso at Purdue University, West Lafayette, Indiana, USA.

^uAlso at Université de Haute Alsace, Mulhouse, France.

^vAlso at Another institute or international laboratory covered by a cooperation agreement with CERN.

^wAlso at University of Hamburg, Hamburg, Germany.

^xAlso at RWTH Aachen University, III. Physikalisches Institut A, Aachen, Germany.

^yAlso at Bergische University Wuppertal (BUW), Wuppertal, Germany.

^zAlso at Brandenburg University of Technology, Cottbus, Germany.

^{aa}Also at Forschungszentrum Jülich, Juelich, Germany.

^{bb}Also at CERN, European Organization for Nuclear Research, Geneva, Switzerland.

^{cc}Also at HUN-REN ATOMKI—Institute of Nuclear Research, Debrecen, Hungary.

^{dd}Also at Universitatea Babeş-Bolyai—Facultatea de Fizica, Cluj-Napoca, Romania.

^{ee}Also at MTA-ELTE Lendület CMS Particle and Nuclear Physics Group, Eötvös Loránd University, Budapest, Hungary.

^{ff}Also at HUN-REN Wigner Research Centre for Physics, Budapest, Hungary.

^{gg}Also at Physics Department, Faculty of Science, Assiut University, Assiut, Egypt.

^{hh}Also at The University of Kansas, Lawrence, Kansas, USA.

ⁱⁱAlso at Punjab Agricultural University, Ludhiana, India.

^{jj}Also at University of Hyderabad, Hyderabad, India.

^{kk}Also at Indian Institute of Science (IISc), Bangalore, India.

^{ll}Also at University of Visva-Bharati, Santiniketan, India.

^{mm}Also at IIT Bhubaneswar, Bhubaneswar, India.

ⁿⁿAlso at Institute of Physics, Bhubaneswar, India.

^{oo}Also at Deutsches Elektronen-Synchrotron, Hamburg, Germany.

^{pp}Also at Isfahan University of Technology, Isfahan, Iran.

^{qq}Also at Sharif University of Technology, Tehran, Iran.

^{rr}Also at Department of Physics, University of Science and Technology of Mazandaran, Behshahr, Iran.

^{ss}Also at Department of Physics, Faculty of Science, Arak University, ARAK, Iran.

^{tt}Also at Helwan University, Cairo, Egypt.

- ^{uu} Also at Italian National Agency for New Technologies, Energy and Sustainable Economic Development, Bologna, Italy.
- ^{vv} Also at Centro Siciliano di Fisica Nucleare e di Struttura Della Materia, Catania, Italy.
- ^{ww} Also at Università degli Studi Guglielmo Marconi, Roma, Italy.
- ^{xx} Also at Scuola Superiore Meridionale, Università di Napoli 'Federico II', Napoli, Italy.
- ^{yy} Also at Fermi National Accelerator Laboratory, Batavia, Illinois, USA.
- ^{zz} Also at Lulea University of Technology, Lulea, Sweden.
- ^{aaa} Also at Consiglio Nazionale delle Ricerche—Istituto Officina dei Materiali, Perugia, Italy.
- ^{bbb} Also at UPES—University of Petroleum and Energy Studies, Dehradun, India.
- ^{ccc} Also at Institut de Physique des 2 Infinis de Lyon (IP2I), Villeurbanne, France.
- ^{ddd} Also at Department of Applied Physics, Faculty of Science and Technology, Universiti Kebangsaan Malaysia, Bangi, Malaysia.
- ^{eee} Also at Trincomalee Campus, Eastern University, Sri Lanka, Nilaveli, Sri Lanka.
- ^{fff} Also at Saegis Campus, Nugegoda, Sri Lanka.
- ^{ggg} Also at National and Kapodistrian University of Athens, Athens, Greece.
- ^{hhh} Also at Ecole Polytechnique Fédérale Lausanne, Lausanne, Switzerland.
- ⁱⁱⁱ Also at Universität Zürich, Zurich, Switzerland.
- ^{jjj} Also at Stefan Meyer Institute for Subatomic Physics, Vienna, Austria.
- ^{kkk} Also at Near East University, Research Center of Experimental Health Science, Mersin, Turkey.
- ^{lll} Also at Konya Technical University, Konya, Turkey.
- ^{mmm} Also at Izmir Bakircay University, Izmir, Turkey.
- ⁿⁿⁿ Also at Adiyaman University, Adiyaman, Turkey.
- ^{ooo} Also at Bozok Universitetesi Rektörlüğü, Yozgat, Turkey.
- ^{ppp} Also at Istanbul Sabahattin Zaim University, Istanbul, Turkey.
- ^{qqq} Also at Marmara University, Istanbul, Turkey.
- ^{rrr} Also at Milli Savunma University, Istanbul, Turkey.
- ^{sss} Also at Informatics and Information Security Research Center, Gebze/Kocaeli, Turkey.
- ^{ttt} Also at Kafkas University, Kars, Turkey.
- ^{uuu} Also at Istanbul Okan University, Istanbul, Turkey.
- ^{vvv} Also at Hacettepe University, Ankara, Turkey.
- ^{www} Also at Istanbul University—Cerrahpasa, Faculty of Engineering, Istanbul, Turkey.
- ^{xxx} Also at Istinye University, Istanbul, Turkey.
- ^{yyy} Also at Yildiz Technical University, Istanbul, Turkey.
- ^{zzz} Also at School of Physics and Astronomy, University of Southampton, Southampton, United Kingdom.
- ^{aaaa} Also at Monash University, Faculty of Science, Clayton, Australia.
- ^{bbbb} Also at Bethel University, St. Paul, Minnesota, USA.
- ^{cccc} Also at Università di Torino, Torino, Italy.
- ^{dddd} Also at Karamanoğlu Mehmetbey University, Karaman, Turkey.
- ^{eeee} Also at California Lutheran University, Thousand Oaks, California, USA.
- ^{ffff} Also at California Institute of Technology, Pasadena, California, USA.
- ^{gggg} Also at United States Naval Academy, Annapolis, Maryland, USA.
- ^{hhhh} Also at Bingol University, Bingol, Turkey.
- ⁱⁱⁱⁱ Also at Georgian Technical University, Tbilisi, Georgia.
- ^{jjjj} Also at Sinop University, Sinop, Turkey.
- ^{kkkk} Also at Erciyes University, Kayseri, Turkey.
- ^{llll} Also at Horia Hulubei National Institute of Physics and Nuclear Engineering (IFIN-HH), Bucharest, Romania.
- ^{mmmm} Also at Another institute formerly covered by a cooperation agreement with CERN.
- ⁿⁿⁿⁿ Also at Hamad Bin Khalifa University (HBKU), Doha, Qatar.
- ^{oooo} Also at Yerevan Physics Institute, Yerevan, Armenia.
- ^{pppp} Also at Imperial College, London, United Kingdom.